

AD-A011 673

STEADY-STATE SOLUTIONS OF A DIFFUSIVE ENERGY-BALANCE
CLIMATE MODEL AND THEIR STABILITY

Michael Ghil

New York University

Prepared for:

Air Force Office of Scientific Research
National Aeronautics and Space Administration
Advanced Research Projects Agency

May 1975

DISTRIBUTED BY:

NTIS

National Technical Information Service
U. S. DEPARTMENT OF COMMERCE

AFOSR - TR - 75 - 796

IMM 410
May 1975

192116

Courant Institute of
Mathematical Sciences

ADA011673

Steady-State Solutions of a Diffusive Energy-Balance Climate Model and Their Stability

Michael Ghil



Sponsored by Advanced Research Projects Agency,
ARPA Order No. 2774 and the
National Aeronautics Space Administration,
NASA-NSG-5034

New York University

Reproduced by
NATIONAL TECHNICAL
INFORMATION SERVICE
U.S. Department of Commerce
Springfield, VA 22151

AIR FORCE OFFICE OF SCIENTIFIC RESEARCH (AFSC)
NOTICE OF TRANSMITTAL TO DDC

This technical report has been reviewed and is
approved for public release IAW AFR 190-12 (7b).
Distribution is unlimited.

D. W. TAYLOR
Technical Information Officer

REPORT DOCUMENTATION PAGE		READ INSTRUCTIONS BEFORE COMPLETING FORM
1. REPORT NUMBER AFOSR - TR - 75 - 0796	2. GOVT ACCESSION NO.	3. RECIPIENT'S CATALOG NUMBER
4. TITLE (and Subtitle) STEADY-STATE SOLUTIONS OF A DIFFUSIVE ENERGY-BALANCE CLIMATE MODEL AND THEIR STABILITY	5. TYPE OF REPORT & PERIOD COVERED Technical	
7. AUTHOR(s) Michael Ghil	6. PERFORMING ORG. REPORT NUMBER	
9. PERFORMING ORGANIZATION NAME AND ADDRESS Courant Institute of Mathematical Sciences New York University 251 Mercer Street, New York, N.Y. 10012	8. CONTRACT OR GRANT NUMBER(s) AFOSR 74-2728 NASA-NSG-5034	
11. CONTROLLING OFFICE NAME AND ADDRESS Advanced Research Projects Agency ⁽¹⁾ National Aeronautics Space Admin. ⁽²⁾	10. PROGRAM ELEMENT, PROJECT, TASK AREA & WORK UNIT NUMBERS ARPA Order 2774	
14. MONITORING AGENCY NAME & ADDRESS (if different from Controlling Office) Air Force Office of Scientific Research, Washington, D.C. ⁽¹⁾ Goddard Inst. of Space Studies, Goddard Space Flight Center, New York, N.Y. ⁽²⁾	12. REPORT DATE May 1975	
	13. NUMBER OF PAGES 79	
	15. SECURITY CLASS (of this report) not classified	
	15a. DECLASSIFICATION SCHEDULE none	
16. DISTRIBUTION STATEMENT (of this Report) Approved for public release; distribution unlimited.		
17. DISTRIBUTION STATEMENT (of the abstract entered in Block 20, if different from Report) none		
18. SUPPLEMENTARY NOTES none		
19. KEY WORDS (Continue on reverse side if necessary and identify by block number) none		
20. ABSTRACT (Continue on reverse side if necessary and identify by block number) We study a diffusive energy-balance climate model, governed by a nonlinear parabolic partial differential equation. Three positive steady-state solutions of this equation are found; they correspond to three possible climates of our planet: an interglacial (nearly identical to the present climate), a glacial,		

and a completely ice-covered earth. We consider also models similar to the main one studied, and determine the number of their steady states. All the models have albedo continuously varying with latitude and temperature, and entirely diffusive horizontal heat transfer. The diffusion is taken to be non-linear as well as linear.

We investigate the stability under small perturbations of the main model's climates. A stability criterion is derived, and its application shows that the "present climate" and the "deep freeze" are stable, whereas the model's glacial is unstable. A variational principle is introduced to confirm the results of this stability analysis.

We examine the dependence of the number of steady states and of their stability on the average solar radiation. The main result is that for a sufficient decrease in solar radiation (about 2 percent) the glacial and interglacial solutions disappear, leaving the ice-covered earth as the only possible climate.

ARPA Order Number: 2774

IMM 410
May 1975

New York University
Courant Institute of Mathematical Sciences

STEADY-STATE SOLUTIONS OF A DIFFUSIVE ENERGY-BALANCE
CLIMATE MODEL AND THEIR STABILITY

Michael Ghil

This research was supported by the Advanced Research Projects Agency under Grant No. AFOSR-74-2728, as well as by the National Aeronautics and Space Administration under Grant No. NASA-NSG-5034.

Views and conclusions contained in this study should not be interpreted as representing the official opinion or policy of the Courant Institute of Mathematical Sciences, or of New York University, or of ARPA.

Approved for public release; distribution unlimited.

Table of Contents

	<u>Page</u>
1. Introduction.....	1
2. The Model.....	5
3. Previous Results.....	12
4. Steady-State Solutions.....	16
5. Stability of the Steady-State Solutions.....	26
a. Stability Criterion.....	32
b. Stability Results.....	36
6. Perturbed Steady-State Solutions and Bifurcation..	41
7. Concluding Remarks.....	47
8. References.....	50
Table Captions.....	53
Tables.....	55
Figure Captions.....	58
Figures.....	61

Acknowledgement

This article contains results of a doctoral dissertation at the Courant Institute of Mathematical Sciences, New York University. The author wishes to thank his advisors, Professors P. D. Lax and E. Isaacson, as well as other members of the Courant Institute too numerous to mention by name. Fruitful conversations with Drs. T. Gal-Chen and S. H. Schneider during a one month stay at the National Center for Atmospheric Research in June 1974 are also gratefully acknowledged. This research was supported in part by the Advanced Research Projects Agency, Grant No. AFOSR-74-2728 and by the National Aeronautics and Space Administration, Grant No. NASA-NSG-5034.

Abstract

We study a diffusive energy-balance climate model, governed by a nonlinear parabolic partial differential equation. Three positive steady-state solutions of this equation are found; they correspond to three possible climates of our planet: an interglacial (nearly identical to the present climate), a glacial, and a completely ice-covered earth. We consider also models similar to the main one studied, and determine the number of their steady states. All the models have albedo continuously varying with latitude and temperature, and entirely diffusive horizontal heat transfer. The diffusion is taken to be nonlinear as well as linear.

We investigate the stability under small perturbations of the main model's climates. A stability criterion is derived, and its application shows that the "present climate" and the "deep freeze" are stable, whereas the model's glacial is unstable. A variational principle is introduced to confirm the results of this stability analysis.

We examine the dependence of the number of steady states and of their stability on the average solar radiation. The main result is that for a sufficient decrease in solar radiation (about 2 percent) the glacial and interglacial solutions disappear, leaving the ice-covered earth as the only possible climate.

1. Introduction

The concept of a climate is one of those abstractions which appears to be self-evident to the layman, but is by no means well defined scientifically. The intuitive idea of a climate has two aspects:

- (a) the most important features of atmospheric phenomena;
- (b) the average behavior of these phenomena over a suitably long time interval and over sufficiently large areas.

The difficulties start when one tries to give a precise meaning to the key words "most important", "suitably long" and "suitably large". We start with "suitably long"; clearly, a year is an absolute lower bound for a reasonable averaging time interval, since daily and seasonal variations should be excluded. To decide over how much longer than a year the averaging should be performed, one has to look at the record. There are three kinds of records: instrumental, the length of which is of the order of hundreds of years, historical, of the order of thousands of years, and geological, of the order of hundreds of thousands of years. These records show that features of the atmosphere change on all the time scales represented in them (e.g., Robinson, 1971). Thus it would appear at first that it is not possible to distinguish between "fast" variations in yearly averages, which should be averaged out when defining a climate, and "slow" variations, which should be considered as "changes

of climate". Still, the geological record seems to indicate that the transitions between considerably colder periods (ice ages or glacials) and warmer periods ("normal" climates or interglacials) occurred over time spans about ten times shorter than the duration of the relatively steady cold or warm weather respectively. This suggests what we shall adopt here as our operative definition of climate, viz., the prevalence of either warm weather (as we experience it today) or of cold weather (to mean a difference of the order of ten degrees centigrade in yearly average below the one recorded in the present).

We turn now to the question of which features of atmospheric phenomena are "most important". Certainly temperature is one of them, not only because its changes left deep traces in the geological record (glaciations in temperate zones, pluviations in the tropics -- SMIC, 1971), but also because it affects all conditions of life and because it is directly linked to the major thermodynamic and dynamic processes in the atmosphere which determine climate and its changes. Also, humidity, wind direction and intensity, cloud amount, precipitation, all play a major role in determining what is perceived as weather and hence should be time-averaged (and, possibly, space-averaged) into climate. Moreover, it is not only the averages of these quantities, but their day-to-night and season-to-season contrast that enters our intuitive concept of a climate.

Thus, at least their variance should be included in a more complete mathematical model for climatology.

In this article we shall treat a very simple model, based on the work of Sellers (1969) and of Schneider and Gal-Chen (1973); we hope that the results will in themselves be of some significance for climate theory, as well as providing insights for devising and analyzing more complex models.

In Section 2 the model to be studied is described; the physical principles on which it is based, as well as the empirical data it uses are discussed.

In Section 3 we discuss the work of different authors on similar models; the similarities and differences between their results are pointed out and the issues arising from these results are outlined.

In Section 4 we compute numerically the model's steady-state solutions of physical interest, i.e., those yielding positive absolute temperatures. Three such solutions, corresponding to three distinct climates of our planet, are obtained: one corresponds to the current climate, the second to an ice age, the third to a completely ice-covered earth. In this section we also explore the effect of certain modifications in the model on the number of steady-state solutions.

In Section 5 the notion of stability for the solutions obtained in Section 4 is defined precisely; it is investigated

using a combination of analytical and numerical techniques. The results are that the present climate and the ice-covered earth are stable, whereas the ice age of the model is unstable.

In Section 6 the effect of changes in the solar radiation on the number and stability of steady-state solutions is studied. The main result is that for a sufficient decrease in the solar radiation (about 2%), the glacial and the interglacial solutions disappear, leaving the ice-covered earth as the only possible climate.

2. The Model

The model chosen for study is a zonally-and-vertically averaged energy-balance climate model. This means that quantities in the model are averaged over longitude and height, leaving colatitude ϕ as the only space variable. The term energy balance means that the model is essentially based on the energy equation of fluid dynamics and has sea-level temperature u as the only dependent variable. The equation governing the model is

$$(1a) \quad C(\phi)u_t = R_i(\phi, u) - R_o(\phi, u) + D(\phi, u, u_\phi, u_{\phi\phi}) ;$$

C is the heat capacity of the atmosphere, land and water masses; R_i is the heat absorbed from incoming radiation,

$$(1b) \quad R_i = Q(\phi)[1 - \alpha(\phi, u)] ,$$

where Q is high-frequency solar radiation and α is the reflectivity (albedo) of the land and sea surface; R_o is the heat lost in outgoing low-frequency planetary re-radiation reaching outer space,

$$(1c) \quad R_o = c(\phi, u)\sigma u^4 ;$$

and D describes the redistribution of heat on the surface of the planet by conduction and convection,

$$(1d) \quad D = \frac{1}{\sin \phi} \frac{\partial}{\partial \phi} [\sin \phi \cdot k(\phi, u)] u_\phi .$$

The coefficients and forcing terms in this model

represent yearly averages of the corresponding quantities and therefore do not depend explicitly on the time t . Averaging the daily and seasonal variations seems justified, since the time scales in which we are interested in our investigation are of the order of hundreds and thousands of years. The lack of explicit dependence on time has the advantage that the model admits, as we shall see, steady-state solutions, $u_t \equiv 0$, which we define to be its climates. The purpose of this work is to study analytically and numerically the number of these climates and their stability under perturbations.

The first model of this type, in finite-difference form and without time dependence, was developed by Sellers (1969). The differential formulation is due to Faegre (1972); time dependence was introduced by Dwyer and Petersen (1973) and, independently, by Schneider and Gal-Chen (1973). Dwyer and Petersen also gave the outline of a systematic derivation of (1) from the energy equation of fluid dynamics, mentioning the main assumptions involved. An even simpler model has been proposed by Budyko (1969): in it the diffusion term D is replaced by a nondifferentiated, linear term in u , and the albedo is a simple step function of u only; this model was also discussed very thoroughly by Leith (1974), and by Held and Suarez (1974).

One of the main features of the model (1a-d) is the form of the albedo,

$$(2a) \quad \alpha = \{b(\phi) - c_1[u_m + (u - c_2 z(\phi) - u_m)_-]\}_c,$$

where the meaning of the subscripts $()_-$ and $\{ \}_c$ is

given for a generic quantity h by

$$(2b) \quad h_- = \min \{h, 0\}$$

and

$$(2c) \quad h_c = \begin{cases} 0.25, & h \leq 0.25, \\ h, & 0.25 < h < 0.85, \\ 0.85, & 0.85 \leq h \end{cases},$$

The subscript c stands for cutoff; the cutoff given by (2c) embodies the observed minimum and maximum values of surface albedo.

Snow and ice have higher reflectivity than bare ground or water; since in regions of lower yearly average temperature the snow and ice cover persists for a longer fraction of the year, at lower temperature the yearly average albedo is higher; this is expressed in the monotonically decreasing dependence of α on u . Further, the plausible assumption is made that, above a certain yearly average temperature u_m , no snow or ice will be present at any time of the year; therefore α is independent of u for $u - c_2 z \geq u_m$, as seen from (2a) and (2b). The term $c_2 z(\phi)$ gives the difference between sea-level temperature u and ground temperature, $u - c_2 z$.

A serious drawback of the model is that it does not include the effect on the albedo of clouds, atmospheric turbidity, relative humidity, and vegetation. The optical properties of these factors and their relationship to surface

temperature are less well known and cannot be easily parameterized in a model as simple as the one at hand.

The factor c in the outgoing infrared radiation term R_0 ,

$$(2d) \quad c = 1 - m \tanh (c_3 u^6) ,$$

expresses empirically the "greenhouse effect", i.e., the screening by the atmosphere, in particular by the clouds in it, of infrared radiation from the earth, thus preventing part of it from reaching outer space. Notice that c decreases as u increases; this indicates that cloud formation, and hence the opacity of the atmosphere to low-frequency radiation, increases with increasing temperature.

The function $k(\phi, u)$ in (1d) has the form

$$(2e) \quad k(\phi, u) = k_1(\phi) + k_2(\phi)g(u) , \quad g(u) = \frac{c_4}{u} e^{-c_5/u} = f'(u) ;$$

$k_1(\phi)u_\phi$ is sensible heat flux in the atmosphere and in the oceans, whereas $k_2(\phi)g(u)u_\phi$ is latent heat flux in the atmosphere. Here $k_1(\phi)$, $k_2(\phi)$ are eddy diffusivities, which parameterize convective transports; true conduction is known to be negligible in the atmosphere-ocean system on the planetary scale. In the original Sellers model, $k(\phi, u)$ had the form

$$k(\phi, u) = k_s(\phi, u) - v(u_\phi) \cdot (u + f(u)) ,$$

where v is, for the purposes of modeling heat flux, mean meridional velocity. The theoretical shortcomings of the

additional term $v \cdot (u + f(u))$ were pointed out by Robinson (1971); the practical difficulties in giving a good parameterization are discussed by Sellers (1973).

Numerical studies of Schneider and Gal-Chen (1973) indicate that results with the original Sellers model (denoted by them as (S)) were very similar to those with the model adopted here (denoted in their work as (SV)), provided that the numerical values of k and k_s were properly chosen (see the discussion on the determination of coefficients further on). Furthermore, the recent work of Gal-Chen and Schneider (1975) shows that there are theoretical grounds on which the formulation (SV) with zero meridional velocity is to be preferred. These considerations will be touched upon later, in a different connection.

The constants c_j , $1 \leq j \leq 5$, u_m , σ , m , as well as the empirical functions $C(\phi)$, $Q(\phi)$, $b(\phi)$, $z(\phi)$, $k_1(\phi)$ and $k_2(\phi)$ are made to fit currently measured values of temperature, radiation, elevation, albedo and heat flux. The functions $C(\phi)$, $Q(\phi)$ and $z(\phi)$ are determined directly from measurements. The function $b(\phi)$ and the constant c_1 in (2a) were computed by Sellers (1969) so as to fit existing albedo measurements in the northern and southern hemisphere. The constants m and c_3 were also computed by Sellers, so as to fit empirical data on R_0 ; σ is the Stefan-Boltzmann constant. The form of the function $g(u)$ and the constants c_4 , c_5 appearing in (2e) are derived from certain physical

considerations having to do with the thermodynamics of wet air and from corresponding empirical data (see Handbook of Meteorology, 1945). The functions $k_1(\phi)$, $k_2(\phi)$ are computed from measured data on sensible and latent heat flux, $k_1(\phi)u_\phi$ and $k_2(\phi)g(u)u_\phi$, respectively. These computations are based on the measured temperature distribution, denoted hereafter by

$$u = \tilde{u}(\phi) ,$$

which will be called the data climate. Note that we use here the term "climate" only for convenience, instead of the lengthier "temperature distribution"; $\tilde{u}(\phi)$ is not necessarily a steady-state solution of the model; we return to this point in Section 4.

The measured data are available at intervals of 10° latitude and are given in Table 1. Since the previously quoted authors used finite-difference formulations with a fixed 10° grid (except Faegre (1972), who used a 5° grid), these data were sufficient for their numerical work. In our numerical work, however, variable grid size was employed, and the 10° data were accordingly fitted by smooth functions. In fact, in order to have an additional check on the well posedness of the model (i.e., the continuous dependence of the solutions on the data, commonly referred to in the meteorological literature as sensitivity), two forms of curve fitting were used: (i) by Bernstein polynomials, and (ii) by cubic splines. Results with the two forms of curve fitting

were indeed very similar (see Table 2).

In this work we only consider symmetric solutions of (1); all data are symmetrized with respect to the equator, $\phi = \pi/2$. For such data the appropriate boundary conditions are

$$(3a) \quad u_{\phi}(0) = 0, \quad (3b) \quad u_{\phi}(\pi/2) = 0;$$

in the symmetric case these are equivalent to $u_{\phi}(0) = u_{\phi}(\pi) = 0$.

We feel that the slight asymmetry between the northern and southern hemispheres could hardly have had a major influence on climatic change. Indeed, the circulations of the two hemispheres are practically separated from each other by the intertropical convergence zone, which acts with respect to our model as an insulating wall. The approximation involved in placing this wall at the equator is no worse than other approximations in the model (see also Held and Suarez, 1974). A further reason for symmetrization will become apparent in the next section.

3. Previous Results

Budyko (1969) and Sellers (1969) used iterative numerical techniques for constructing solutions of their time-independent models. They explored a range of values of the parameters appearing in the model, especially of the solar radiation Q , and obtained one solution for each set of values. These solutions did not depend smoothly on the parameter values; in several instances, small changes in the parameters led to large changes in the solution. For instance, an increase or decrease of a few percent in Q resulted in temperature changes leading to extensive melting, or significant expansion of the polar cap, respectively.

Faegre (1972) obtained for a certain given set of values of the parameters five distinct solutions of his variant of the Sellers time-independent model. Two of these were highly asymmetric, and disappeared when $c(\phi, u)$ in (1) was taken as constant; hence Faegre considered these solutions to be spurious and unphysical. It was the desire to eliminate a priori such solutions that suggested the choice of symmetric coefficients. Faegre's formulation of the albedo is slightly different from that of Sellers, mainly in that the minus subscript in (2a) (i.e., the cutoff of $\alpha(\phi, u)$ at u_m) was missing.

The three symmetric solutions of Faegre could be described as corresponding to the present climate, an

ice-age climate (about 15° C colder on the average than the previous one), and a completely ice-covered earth (at an average temperature of about 175 K). This last climate was also the one obtained by Sellers when decreasing the solar radiation by more than 4%.

These results raised the question of the transitivity of the earth's climate, as formulated by Lorenz (1968, 1970). In Lorenz's terminology, a time-dependent system of equations is transitive if its solutions have a unique equilibrium statistic, that is, if all solutions, independently of initial conditions, have the same infinite time average; otherwise the system is intransitive. Lorenz pointed to the existence of certain transitive systems which possess a property called by him almost intransitivity, i.e., that of having at least some solutions whose averages over long, but finite, time intervals are different -- these solutions then would alternate in time between the different averages. He raised the possibility that the atmospheric system is almost intransitive; in other words, that the known climate changes in the past were not necessarily caused by changes in external conditions (like solar radiation), but rather were an effect of the normal evolution of the system.

Schneider and Gal-Chen (1973) investigated the question of transitivity for energy-balance climate models by formulating time-dependent versions of the Budyko (B), Sellers (S and SV) and Faegre (F) models. They solved

numerically the initial-value problem governing these time dependent models for a large range of initial conditions. The models were found to be intransitive, rather than almost intransitive: every solution tended as $t \rightarrow \infty$ to one of two (or more, in the case of the (F) model) equilibrium solutions; viz., the equilibrium statistic of the system governing each model was not unique, and no spontaneous transition from one equilibrium to another was possible. The two equilibrium solutions obtained for all models corresponded to the present climate and to the previously mentioned completely ice-covered earth.

The equilibrium solutions, at least for the (S) and (SV) models, proved stable under rather large perturbations in both initial conditions and parameters. That is, solutions which differed in their initial conditions from one of the limiting "equilibria" by as much as ± 18 K tended as $t \rightarrow \infty$ to the "equilibrium" near which they started. Also changes of $\pm 1.5\%$ in the solar radiation led to limiting equilibria which differed by only a few degrees from the unperturbed ones. However, changes of more than -18 K in initial conditions or -1.5% in solar radiation led from the "present climate" to the "ice-covered earth". The latter seemed to be the most stable climate in all investigations mentioned above.

Schneider and Gal-Chen did not obtain a limiting steady-state solution which would correspond to a true ice age as

recorded in the planet's history. Their results with the time-dependent version of the Faegre model (F) were rather different from those with the two versions of the Sellers model (S and SV), especially with regard to the stability of steady states under perturbations.

Contrary to the results of Schneider and Gal-Chen, Dwyer and Petersen (1973), with a time-dependent model essentially identical to Schneider and Gal-Chen's (S), obtained solely one type of limiting steady state, that corresponding to the "present climate". They used only the data climate $u = \tilde{u}(\phi)$ as initial conditions, but varied the solar radiation Q . The actual values of the limiting equilibrium depended of course on the values of Q used, but slight changes in Q yielded only a difference of a few degrees between the average temperature of the equilibrium and that of the data climate; no "deep freeze" equilibrium was obtained.

These results seemed to be interesting enough in order to warrant further study of energy-balance climate models. As indicated in the previous section we chose to investigate symmetric solutions of the (SV) model of Schneider and Gal-Chen, and of some variations thereof, including the (F) model. We hope that this study will add as much light and as little heat as possible to the climate question (Jackson, 1962).

4. Steady-State Solutions

We turn now to the mathematical theory of equation (1). Introducing the new space variable $x = 2\phi/\pi$, we obtain the initial-and-boundary value problem (IBVP);

$$\begin{aligned} C(x)u_t = & \left(\frac{2}{\pi}\right)^2 \frac{1}{\sin(\pi x/2)} \frac{\partial}{\partial x} \sin \frac{\pi x}{2} \cdot [k_1(x) + k_2(x)g(u)]u_x \\ & - \sigma u^4 [1 - m \tanh(c_3 u^6)] \\ (4) \quad & + \mu Q(x) \left\{ 1 - b(x) + c_1 [u_m + (u - c_2 z(x) - u_m) -] \right\}_c, \end{aligned}$$

$$0 < x < 1, \quad 0 < t,$$

$$(5a) \quad u_x(0, t) = u_x(1, t) = 0, \quad (5b) \quad u(x, 0) = \bar{u}(x),$$

where (4) is a nonlinear parabolic partial differential equation (PDE). Here $g(u)$ is given by (2e), $\mu = 1$ (its significance will appear later, in Section 6) and

$$\begin{aligned} c_1 &= 0.009, \quad c_2 = 0.0065 \text{ deg m}^{-1}, \quad c_3 = 1.9 \times 10^{-15} \text{ deg}^{-6}, \\ (6) \quad c_4 &= 6.105 \times 0.75 \times \exp(19.6) \times 10^3 \text{ dyn deg cm}^{-2}, \quad c_5 = 5350 \text{ deg}, \\ \sigma &= 1.356 \times 10^{-12} \text{ cal cm}^{-2} \text{ sec}^{-1} \text{ deg}^{-4}, \quad m = 0.5, \quad u_m = 283.16 \text{ deg}. \end{aligned}$$

Mesh data at 10° latitude for $C(x)$, $k_1(x)$, $k_2(x)$, $Q(x)$, $b(x)$, $z(x)$ are given in Table 1. The units of the constants and

mesh data are chosen such that the common units of all terms in (4) are $\text{cal cm}^{-2}\text{sec}^{-1}$.

The first step of the investigation is to find steady-state solutions of (4, 5a) in the range of physical interest, and to study their dependence on changes in the model. We consider therefore the steady-state equation obtained from (4) by setting $u_t \equiv 0$. After some rearrangement we get the following two-point boundary-value problem (BVP) for the system of ordinary differential equations (ODE):

$$(7a) \quad u_x = v ,$$

$$(7b) \quad v_x = - \left(\frac{\pi}{2}\right)^2 \frac{F(x,u)}{k(x,u)} - \frac{\pi}{2} \left(\cot \frac{\pi x}{2}\right) v - \frac{k_1'(x) + k_2'(x)g(u)}{k(x,u)} v - \frac{k_2(x)g'(u)}{k(x,u)} v^2 , \quad 0 < x < 1 ,$$

$$(8) \quad v(0) = v(1) = 0 ,$$

where

$$(7c) \quad k(x,u) = k_1(x) + k_2(x)g(u) ,$$

$$(7d) \quad F(x,u) = \mu Q(x) \left\{ 1 - b(x) + c_1 [u_m + (u - c_2 z(x) - u_m)_-] \right\} c - \sigma u^4 [1 - m \tanh(c_3 u^6)] .$$

We use shooting (Isaacson and Keller, 1966, Keller, 1968) as the numerical procedure to solve (7, 8): equations (7a,b)

are solved with initial conditions

$$(9a) \quad v(0) = 0 ,$$

$$(9b) \quad u(0) = u_0 ,$$

for different values of u_0 ; denote by $u(x;u_0)$, $v(x;u_0)$ the solution of the initial-value problem (IVP) (7,9) in order to emphasize its dependence on the parameter u_0 . An iterative scheme is then used to obtain those values of u_0 which satisfy

$$(10) \quad v(1;u_0) = 0 .$$

For these values of u_0 the solution $u(x;u_0)$, $v(x;u_0)$ of the IVP (7,9) is also a solution of the BVP (7,8).

To obtain numerical solutions of prescribed accuracy to the BVP (7,8) one has therefore (Keller, 1968) to achieve the desired accuracy both in

- (i) solving the IVP (7,9), and in
- (ii) solving iteratively the nonlinear (finite) equation (10).

In solving numerically the IVP (7,9), we encounter the difficulty that (7b) is singular at the origin, since $\cot(\pi x/2) \rightarrow \infty$ as $x \rightarrow 0$. This singularity arises from the mathematical form of the diffusion term D of (1) in spherical coordinates. It is easily shown, though, that (analytical) solutions of the IVP exist and are unique at least "in the small", i.e., for $|u_0 - U_0| < \epsilon$, $0 < x < \delta$, arbitrary U_0 and some $\delta, \epsilon > 0$. The numerical difficulty of the initial point being singular can be circumvented by using a variable-step method.

It also turns out that in order to achieve prescribed over-all accuracy of the numerical solution of (7,9) with a minimum of computational effort it is convenient to use a variable-step variable-order multistep scheme. The ODE solver we computed with was developed at the Lawrence Livermore Laboratory and is documented by Hindmarsh (1972,1974). Both the Gear and Adams methods included in the package were used and gave results identical to within the prescribed relative accuracy, which was 10^{-7} ; however, the Adams method was faster and was therefore used in most integrations.

The number of steps needed per solution (per value of u_0) for this accuracy was of the order of 100. It is of interest to point out that near the singularity at $x = 0$, and near the point where the jump discontinuity in the derivative of $F(x, u(x; u_0))$ occurred, the order of accuracy chosen by the scheme was one and the step size was very small, so that a proportionately larger amount of computation was done in the neighborhood of these two points.

Thus every solution of (7,9) for given u_0 puts at our disposal a value of the function $v(1; u_0)$, accurate to 10^{-4} .^{*} To find the zeros of $v(1; u_0)$, we used the method of false position (Isaacson and Keller, 1966). The criterion for u_0 to be a root of (10) was $|v(1; u_0)| < 10^{-3}$.

^{*} In the units chosen, typical values of u are $O(10^3)$ and of v are $O(10^2)$.

The range of physical interest in which we searched for solutions of (10) was $100K \leq u_0 \leq 300K$ (see also Faegre, 1972). Within this range, three solutions of the BVP (7,8) were found which are denoted by $u_1(x)$, $u_2(x)$, $u_3(x)$. They correspond to

$$u_1(0) = 247.74 K, \quad u_2(0) = 223.97K, \quad u_3(0) = 168.94 K.$$

The curve $u_x(1)$ vs. $u(0)$, the zeros of which correspond to the solutions u_3, u_2, u_1 , is given in Figure 2. The individual solutions $u_1(x)$, $u_2(x)$, $u_3(x)$ are plotted in Figure 3.

It is customary and useful to characterize a climate of the model, i.e., one of the solutions above, by its average temperature, rather than by the temperature at the pole. Therefore we introduce for functions ϕ the averaging operator $\bar{\cdot}$ by

$$\bar{\phi} = \frac{\int_0^2 \phi(x) \sin\left(\frac{\pi x}{2}\right) dx}{\int_0^2 \sin\left(\frac{\pi x}{2}\right) dx}.$$

In particular, it is known (Isaacson and Keller, 1966) that for functions ϕ symmetric about the equator, $\phi(2-x) = \phi(x)$, which also satisfy $\phi_x(0) = 0$, and hence can be extended so as to have period 2, the trapezoidal-quadrature approximation of $\bar{\cdot}$ is very accurate. Denote this approximation by $\bar{\cdot}_\Delta$, where $\Delta = 1/9$ (corresponding to a 10° mesh); then we have

$$\bar{\cdot}_\Delta u_1 = 287.76 K, \quad \bar{\cdot}_\Delta u_2 = 267.44 K, \quad \bar{\cdot}_\Delta u_3 = 175.43 K.$$

Clearly u_1 corresponds to an interglacial, u_2 to a glacial, and u_3 to the ice-covered earth.

Note that for the data climate $u = \tilde{u}(x)$

$$\tilde{u}(0) = 247.36 \text{ K}, \quad \epsilon_{\Delta} \tilde{u} = 287.20 \text{ K},$$

which is indeed very close to the interglacial solution of the model, u_1 (see also Figure 3). Though present observations were used to obtain constants and empirical functions in (4), no explicit term was added to ensure that (4) hold with $u_t \equiv 0$; also the diffusion term, D , is of the same order of magnitude as the radiation terms, R_i and R_0 , so that this is not the result of a simple radiation balance. The same is true of the work of all the previous authors discussed in Section 3^{*}; these authors, however, assumed at least implicitly that the data climate should be a steady-state solution of the model, or approximately so. Since this result is not actually built into the model, as far as we can see, we think it is rather remarkable that this class of models yields a steady-state solution, $u_1(x)$, very close to the data climate, $\tilde{u}(x)$. Henceforth we shall refer to u_1 also as the "present climate" of the model.

* In fact, Schneider and Gal-Chen (1973) did use an extra "fudge coefficient", $0.97 \leq c_0(x) \leq 1.03$, in R_0 in order to achieve better agreement between the interglacial, or "present" climate of their models and the data climate; they obtained $\epsilon u_1 \approx 287.06 \text{ K}$ vs. $\epsilon \tilde{u} \approx 287.30 \text{ K}$ for the (S) model.

The mesh data, from which constants and empirical functions for the model were computed, are known to be in error by possibly as much as 100% (Schneider and Gal-Chen, 1973); also some of the parameterizations used in formulating the model are questionable. Therefore we made a number of computations in order to obtain information on the dependence of the physically significant solutions, u_1, u_2, u_3 , on variations in the model. The salient features of these computations, summarized in Table 2, are:

(1) The dependence of all these solutions on the coefficients seems to be very smooth.

(2) The bounds on the albedo, $0.25 \leq \alpha(x, u) \leq 0.85$, are essential for the existence of three steady-state solutions in the physical range, $100 \text{ K} \leq u(0) \leq 300 \text{ K}$: u_3 disappears when the bound $\alpha \leq 0.85$ is not enforced, and u_1 disappears when the bound $0.25 \leq \alpha$ is not enforced.

(3) The terrestrial radiation term R_0 , given by (1c), and its nonlinearity are essential for the existence of physically significant solutions: if the term is set equal to zero all solutions, u_1, u_2, u_3 , disappear; when it is replaced by its average,

$$R_0 \equiv \epsilon_{\Delta} c(x, \tilde{u}(x)) \sigma \tilde{u}^4(x) = \text{const.} ,$$

u_2 only obtains; when R_0 is replaced by a linear approximation,

$$R_0 = \sigma \bar{u}^3 \{ \bar{u} + 4(u - \bar{u}) \} \epsilon_{\Delta} c(x, \tilde{u}(x)) , \quad \bar{u} = \epsilon_{\Delta} \tilde{u}(x) ,$$

then u_1 only obtains.

(4) Our results with the model using the Faegre formulation of the albedo are very similar to those using the Sellers formulation; it is hard to explain the disagreement in this respect between our results and those of Schneider and Gal-Chen (1973), who, as mentioned in Section 3, obtained very different results when using the two albedo formulations.

(5) The values of the empirical functions in the model when fitting mesh data by (i) Bernstein polynomial approximation and (ii) cubic spline interpolation are pointwise rather different for some of the functions (see Figure 1). The solutions of (7,8) when using these different fits are, however, very close. This also supports the assertion in paragraph (1) above, and shows that the uncertainty in the mesh data does not affect in an important way the conclusions of the investigation.

We explored another variant of the model, in which the eddy diffusivity $k(x,u)$ given in (7c), corresponding to the (SV) model of Schneider and Gal-Chen, was replaced by $k(x,\tilde{u})$, where \tilde{u} is the data climate; hence also $g'(u)v$ in (7b) is replaced by $g'(\tilde{u})\tilde{u}'(x)$. This variant, in accordance with the terminology of Gal-Chen and Schneider (1975), would correspond to an (SVC) model. We denote this modification of (7) by (7'); the solutions of (7',8) are

$$u_1(0) = 247.55 \text{ K}, \quad u_2(0) = 227.76 \text{ K}, \quad u_3(0) = 169.44 \text{ K},$$

$$\Delta u_1 = 287.70 \text{ K}, \quad \Delta u_2 = 268.60 \text{ K}, \quad \Delta u_3 = 175.44 \text{ K}.$$

These are indeed very close to the solutions of (7,8), especially for u_1 and u_3 (see also Figure 3).

Gal-Chen and Schneider (1975) investigated the effect of variations in the solar radiation μQ on the equator-to-pole temperature gradient; they argue that this dependence should be monotone, in fact monotone increasing. In the light of this argument and of their results, model (SV) is superior to (S), as already mentioned in Section 2; moreover, model (SVC) is superior to (SV). Since (SVC) is also more convenient to use when investigating the stability of the steady-state solutions, we shall work with it in the sequel; the corresponding form of (4) we denote by (4'), the corresponding form of (1) by (1'), and the corresponding form of (7) by (7').

For this model, additional computations were made outside the range of physical interest. One more steady-state solution was found; we denote it by $u_4(x)$, and it satisfies

$$u_4(0) = -185.99 \text{ K}, \quad \varepsilon_{\Delta} u_4 = -175.40 \text{ K}.$$

Most probably there are no other solutions of the BVP (7',8) at all. Indeed, the solutions of the IVP (7',9) become unbounded as u_0 moves towards the ends of the range explored, viz., $-1330 \text{ K} \leq u_0 \leq 300 \text{ K}$; i.e., $u(x;u_0) \rightarrow +\infty$ as u_0 approaches the ends of the interval above (see Figure 2).

We would like also to point to the fact that some of the modifications of the model which have three physical steady states yielded numerical values of the latter consider-

ably higher than u_1, u_2, u_3 (see Table 2); however, it was the qualitative feature of the number of solutions and their approximate position with respect to each other that was of interest in our investigation: the average temperature of a given solution of any fixed model could be changed to practically coincide with that of the solution u_j of (4) to which it corresponds by adjusting the values of the coefficients.

5. Stability of the Steady-State Solutions

In the previous section we have shown that equation (4') with the boundary conditions (5a) has three steady-state solutions of physical interest, $u = u_j(x)$, $1 \leq j \leq 3$. In this section we shall study the stability of these steady states.

Let us concentrate on any one of the steady states above, $u = u_j(x)$, where j is fixed. Stability of u_j means that small perturbations of u_j die out with time. More precisely, u_j is stable if, when taking any nearby state $\overset{\circ}{U}$, i.e., one which differs little from u_j ,

$$(11) \quad \overset{\circ}{U} = u_j(x) + \varepsilon \overset{\circ}{v}(x),$$

say, where $\overset{\circ}{v}$ is arbitrary and $\varepsilon > 0$ is not too large, then the solution $U(x, t; \varepsilon)$ of (4'-5) with initial condition $U(x, 0; \varepsilon) = \overset{\circ}{U}(x; \varepsilon)$ tends to u_j itself as $t \rightarrow \infty$.

Let (4') be written symbolically as

$$(12) \quad u_t = N(u),$$

where we divided through equation (4') by $C(x)$, $0 < C_m \leq C(x) \leq C_M < \infty$, and $N(u)$ is the corresponding right-hand side. Take a perturbed u , $u = U(x, t, \varepsilon)$, which is assumed to satisfy the boundary conditions (5a) and the initial condition (11). If such a solution of (12) exists for all ε sufficiently small, $0 < \varepsilon \leq \varepsilon_0$, then the equations

$$(12') \quad \frac{U_t(x,t;\varepsilon) - U_t(x,t;0)}{\varepsilon} = \frac{N(U(x,t;\varepsilon)) - N(U(x,t;0))}{\varepsilon},$$

$$0 < \varepsilon \leq \varepsilon_0,$$

also hold, with $U(x,t;0) = u_j(x)$. Letting $\varepsilon \rightarrow 0$ we obtain the linearized equation

$$(13a) \quad v_t = -L_j v,$$

where we define $v(x,t) \equiv \frac{\partial}{\partial \varepsilon} U(x,t;\varepsilon)|_{\varepsilon=0}$ and

$$(13b) \quad L_j = - \frac{\partial}{\partial \varepsilon} N(U(x,t;\varepsilon))|_{\varepsilon=0} = - \frac{\partial}{\partial u} N(u)|_{u=u_j}, \quad 1 \leq j \leq 3.$$

At this point, for the sake of simplicity, we shall drop the subscript j , and u will thus stand for some u_j , L for the corresponding L_j .

Equation (13a) is linear in v and it has a unique solution v satisfying the boundary conditions

$$(13c) \quad v_x(0,t) = v_x(1,t) = 0,$$

and arbitrary initial conditions

$$(13d) \quad v(x,0) = \overset{\circ}{v}(x).$$

The solution may be found by the usual method of separation of variables, or expansion in eigenfunctions (normal modes).

Consider

$$v(x,t) = e^{-\lambda t} w(x);$$

this v will be a solution of (13) with $v(x,0) = w(x)$ iff (if and only if) λ is an eigenvalue and w is an eigenfunction of L , i.e., iff the pair (λ, w) satisfies the homogeneous problem

$$(14a) \quad Lw = \lambda w$$

$$(14b) \quad w_x(0) = w_x(1) = 0.$$

We shall show that the operator L has sufficiently many eigenfunctions, and that therefore any solution v of (13) can be written as a series

$$(15) \quad v(x,t) = \sum_{k=0}^{\infty} a_k e^{-\lambda^{(k)} t} w^{(k)}(x)$$

where $(\lambda^{(k)}, w^{(k)})$ are all the solutions of (14). It is clear from the derivation (12') of (13) and from (15) that for the steady state u to be stable it is necessary that every eigenvalue $\lambda^{(k)}$ of L have positive real part:

$$(16) \quad \operatorname{Re} \lambda^{(k)} > 0.$$

This condition defines the so-called linear stability of u . It has been shown rigorously in a few cases and it is believed in many others that (16) is also sufficient for the stability of u as we defined it at the beginning of this section, i.e., that linear stability implies nonlinear stability. In the next section we shall give an argument which will make it at least plausible that this is the case also for the problem at hand.

We turn now to the analysis of the eigenvalues of the linear second-order ordinary differential operator L , which we can write as

$$(17a) \quad Lw = - \frac{1}{r(x)} (p(x)w_x)_x + q(x)w .$$

Here p, q, r are determined by (13b) and by (4'):

$$(17b) \quad r(x) = C(x) \sin \left(\frac{\pi x}{2} \right) ,$$

$$(17c) \quad p(x) = \left(\frac{2}{\pi} \right)^2 \sin \left(\frac{\pi x}{2} \right) \cdot k(x, \tilde{u}) ,$$

$$(17d) \quad q(x) = \{Q(x)(c_1)_{c'} - d(x, u)\} / C(x) ,$$

with

$$(17e) \quad (c_1)_{c'} = \begin{cases} c_1 & \text{if } 0.25 \leq \alpha(x, u) \leq 0.85 \\ & \text{and } u(x) - c_2 z(x) - u_m \leq 0 , \\ 0 & \text{otherwise,} \end{cases}$$

and

$$(17f) \quad d(x, u) = \frac{\partial}{\partial u} c(x, u) \sigma u^4 \\ = \sigma u^3 \left\{ 4[1 - m \tanh(c_3 u^6)] - 6mc_3 u^6 [1 - \tanh^2(c_3 u^6)] \right\} .$$

Clearly L thus defined is formally self-adjoint (Courant and Hilbert, 1953, Birkhoff and Rota, 1969) under the prescribed boundary conditions with respect to the inner product

$$(18) \quad (w_1, w_2) = \int_0^1 r(x) w_1(x) w_2(x) dx .$$

Moreover, r, p are nonnegative and twice continuously differ-

entiable on the interval $I = [0,1]$, and q is piecewise continuous on I . However, because of the singularity at $x = 0$ due to the fact that $r(0) = p(0) = 0$, the usual Sturm-Liouville theory of self-adjoint operators (Courant and Hilbert, 1953, Birkhoff and Rota, 1969) does not apply to L ; this difficulty though can be overcome and the theory can be extended. The crucial element in this extension is the observation that, because of the boundedness of q , L is bounded from below in the sense that, for any w satisfying (14b) for which $(w,w) < \infty$, the inequality

$$(19a) \quad \langle w, w \rangle \geq K(w, w) ,$$

holds with some fixed constant K , $K \geq \min_{0 \leq x \leq 1} q(x) > -\infty$, independent of w ; here $\langle w, w \rangle$ is the Dirichlet integral corresponding to L ,

$$(19b) \quad \langle w, w \rangle \equiv (Lw, w) = \int_0^1 (pw_x^2 + rqw^2) dx .$$

This result, together with an analysis of the nature of the singularity at $x = 0$, are sufficient to show that indeed L has a complete system of eigenfunctions, orthonormal with respect to the inner product (18) (Birkhoff and Rota, 1969), and that the eigenvalues of L are real and can be arranged in an ascending sequence

$$-\infty < \lambda^{(1)} \leq \lambda^{(2)} \leq \lambda^{(3)} \leq \dots$$

with $\lambda^{(k)} \rightarrow \infty$ as $k \rightarrow \infty$, and $K = \lambda^{(1)}$ in (19). Hence any solution v of (13) can be written as a series (15).

Therefore the stability question for the steady state u reduces to determining whether

$$(16') \quad \lambda^{(1)} > 0 ,$$

in which case u is stable, or whether the opposite holds, in which case u is unstable.

5a. Stability Criterion

In this subsection we shall show that it is possible to determine the sign of $\lambda^{(1)}$ without actually computing $\lambda^{(1)}$.

We start with the variational characterization of the lowest eigenvalue (Courant and Hilbert, 1953), $\lambda^{(1)}$,

$$(20) \quad \lambda^{(1)} = \min_{\substack{\langle v, v \rangle < \infty \\ (v, v) \neq 0}} \frac{\langle v, v \rangle}{(v, v)} = \min_{(v, v) = 1} \langle v, v \rangle ,$$

i.e., $\lambda^{(1)}$ is the minimum of the Rayleigh quotient $R(v)$ corresponding to L ,

$$(21) \quad R(v) \equiv \langle v, v \rangle / (v, v) ,$$

and the minimum is assumed for $v = w^{(1)}$. Indeed, (14a) is the Euler equation for (20), and $v_x(1) = 0$ is the "natural" boundary condition for (20) in the sense of the calculus of variations (Courant and Hilbert, 1953); also $v_x(0) = 0$ is, according to the theory of singular operators with the properties of L , the only boundary condition at $x = 0$ which ensures that, for solutions v of (14), $\langle v, v \rangle$ as well as (v, v) is finite. In particular, we conclude that the minimizing function, $v = w^{(1)}$, is at least as smooth as the coefficients of L , viz., it must have a piecewise continuous second derivative.

With these preliminaries we are able to prove the following known

Lemma. The first eigenfunction of L , $w^{(1)}$, is strictly positive,

$$w^{(1)}(x) > 0, \quad 0 \leq x \leq 1.$$

Proof: From the definition (21) of $R(v)$ it is clear that

$$R(|w^{(1)}|) = R(w^{(1)}),$$

where $|y|$ denotes the absolute value of y . If $w^{(1)}$ had a zero at some interior point x_0 , $0 < x_0 < 1$, and $w_x^{(1)}(x_0) \neq 0$, then the first derivative of $|w^{(1)}|$ would have a jump at $x = x_0$, which contradicts the smoothness of $|w^{(1)}|$ as a solution of the variational problem. If, on the other hand, $w_x^{(1)}(x_0) = 0$, $0 < x_0 < 1$, or $w^{(1)}(0) = 0$, or $w^{(1)}(1) = 0$, then, by the uniqueness theory of linear ODE (Birkhoff and Rota, 1969), it would follow that $w^{(1)} \equiv 0$; this contradicts the fact that $w^{(1)}$ is a nontrivial solution of (14), completing our proof.

Now we are ready to state our stability criterion, which is part of the conclusion of the

Theorem. Let L , $\lambda = \lambda^{(1)}$, $w = w^{(1)}$ be as above. Suppose also that there exists a function v , as smooth as w , nonnegative, $v \geq 0$ on I , and satisfying

$$(22) \quad Lv \geq 0, \quad v_x(0) = 0, \quad v(0) = 1.$$

Then $v_x(1) \geq 0$ implies $\lambda \geq 0$. Moreover,

- (i) $\lambda > 0$ if either $Lv \not\equiv 0$ or $v_x(1) > 0$, and
- (ii) if $Lv \equiv 0$ holds, then $\lambda > 0$, $\lambda = 0$, or $\lambda < 0$, according to whether $v_x(1) > 0$, $v_x(1) = 0$, or $v_x(1) < 0$.

Proof: The required results are easily read off from the following sequence of equalities obtained from the definitions and by integration by parts:

$$\begin{aligned}
 \lambda \int_0^1 r v w &= \lambda (w, v) = (Lw, v) = \int_0^1 -(pw_x)_x v + rqwv \\
 &= -pw_x v \Big|_0^1 + \int_0^1 pw_x v_x + rqwv \\
 &= pwv_x \Big|_0^1 + \int_0^1 -(pv_x)_x w + rqvw \\
 &= (pwv_x)(1) + (Lv, w) ,
 \end{aligned}$$

where we used $w_x(0) = w_x(1) = 0$ and $v_x(0) = 0$.

Note. This is essentially a comparison theorem, of the type familiar from Sturm-Liouville theory (Birkhoff and Rota, 1969).

The result under (ii) above is the stability criterion which we shall use. For completeness we give here also the following slight generalization as a

Corollary. Let L, λ, w be as in the Theorem. Suppose v satisfies the hypotheses of the theorem, except for that of being nonnegative on I . Instead, let x_0 , $0 < x_0 \leq 1$, be the first zero of v ,

$$v(x) > 0 \quad \text{on} \quad 0 \leq x < x_0.$$

Then $\lambda < 0$.

Proof: The result follows from the same integration by parts carried out in the proof of the theorem, except that now the upper limit of integration has to be x_0 rather than 1, and we use $v(x_0) = 0$ rather than $w_x(1) = 0$ in passing from the second to the third line. Moreover, since $v(x) > 0$ for $x < x_0$, and v is continuously differentiable, $v_x(x_0) \leq 0$. Furthermore, it cannot be that both $Lv \equiv 0$ and $v_x(x_0) = 0$, since then we would have, by uniqueness, $v \equiv 0$, which contradicts $v(0) = 1$. This completes the proof.

5b. Stability Results

In this subsection we shall apply the stability criterion obtained in Subsection 5a to the steady-state solutions u_j , $1 \leq j \leq 3$.

For this purpose we construct functions v_j by solving (22) with the equality sign, and with $L = L_j$ given by (13b) and (17). The results, obtained with a relative numerical accuracy of 10^{-7} , are that

- (a) v_j , $j = 1, 2, 3$, is positive, $v_j \geq V_j > 0$, $V_j \geq 0.5$;
- (b) $\frac{d}{dx} v_j(1) > 0$ for $j = 1, 3$, whereas $\frac{d}{dx} v_j(1) < 0$ for $j=2$.

The actual computed values are

$$\frac{d}{dx} v_1(1) = 2.39970, \quad \frac{d}{dx} v_2(1) = -3.24312, \quad \frac{d}{dx} v_3(1) = 4.31025.$$

These values of the derivatives at $x = 1$, together with the values of V_j , are sufficiently bounded away from zero in order to conclude that the conditions of the theorem are satisfied beyond the doubt of numerical uncertainty.

Hence the solutions representing the present climate and the ice-covered earth are stable, whereas the so-called ice age of the model is unstable. This result agrees with and throws additional light on the results of previous authors, in particular the time-dependent integrations of Schneider and Gal-Chen (1973).

Actually the stability computations were carried out also for the solutions of

$$(4'') \quad N'(u_j) = 0, \quad 1 \leq j \leq 3,$$

with

$$(23) \quad N'(u) = \left(\frac{2}{\pi}\right)^2 \frac{K_0}{\sin(\pi x/2)} \frac{\partial}{\partial x} \sin\left(\frac{\pi x}{2}\right) \cdot u_x \\ + Q(x) \left\{ 1 - B_0 + c_1 u \right\}_c - c_6 \sigma u^4,$$

where the subscript $\left\{ \right\}_c$ is defined in (2c) and

$$K_0 = \varepsilon_{\Delta} k(x, \tilde{u}(x)) = 2.2 \times 10^{-5}, \quad B_0 = \varepsilon_{\Delta} b(x) = 2.85881,$$

$$c_6 = \varepsilon_{\Delta} c(x, \tilde{u}(x)) = 0.61;$$

the corresponding linearization of N' is

$$(13') \quad L'_j = -N_u(u_j) = \left(\frac{2}{\pi}\right)^2 \frac{K_0}{\sin(\pi x/2)} \frac{\partial}{\partial x} \sin\left(\frac{\pi x}{2}\right) \frac{\partial}{\partial x} \\ + Q(x) (c_1)_c'' - 4c_6 \sigma u_j^3,$$

where

$$(c_1)_c'' = \begin{cases} c_1 & \text{if } 0.25 \leq 1 - B_0 + c_1 u_j \leq 0.85, \\ 0 & \text{otherwise} \end{cases}$$

This is, according to the experiments carried out in Section 4 (see Table 2), the simplest form of (4) which still yields approximately the same steady-state solutions in the physical range of interest. The results are the same, i.e., u_1 and u_3

are stable, and u_2 is unstable. It seems therefore quite plausible to conclude also that for all models, lying in some sense between (4) and (4''), the steady states corresponding roughly to u_1, u_2, u_3 have the same stability properties as the latter. Combining this remark with the one made at the end of Section 4, it seems that we have a result about the stability of the steady states for a certain type of energy-balance model, rather than just for one specific model of this type. It seems desirable to define precisely the type of model having these properties, and we intend to try to do so in further work.

Having thus determined the stability properties of the steady states of (4'), we want to obtain some additional information by actually computing the lowest eigenvalues $\lambda_j^{(1)}$, and corresponding eigenfunctions $w_j^{(1)}$, of L_j , $1 \leq j \leq 3$. The eigenvalues are

$$\lambda_1^{(1)} = 3.95390 \times 10^{-9}, \quad \lambda_2^{(1)} = -5.87662 \times 10^{-9}, \quad \lambda_3^{(1)} = 5.13587 \times 10^{-9},$$

and the eigenfunctions $w_j^{(1)}$, $1 \leq j \leq 3$ are plotted in Figure 4.

The method for computing $(\lambda_j^{(1)}, w_j^{(1)})$ was again shooting, this time with respect to the parameter λ . That is, equation (14a) with $L = L_j$, was solved for $w(x; \lambda)$ with initial conditions

$$w(0; \lambda) = 1, \quad w_x(0; \lambda) = 0,$$

and with different values of the "shooting parameter" λ . The zeros of the function $v_x(1; \lambda)$ were then computed by regula falsi to within an accuracy of 10^{-4} . The over-all relative error in computing solutions of the initial-value problem was 10^{-7} , as before.

Notice from (15) that

$$\tau = 1/|\lambda_j^{(1)}|$$

is a characteristic decay or relaxation time for the solution $U(x,t;\varepsilon)$ of (12) to $u = u_j(x)$. This time is of the order of 10 years for all j ,

$$\tau_1 \approx 8.0 \text{ years} , \quad \tau_2 \approx 5.4 \text{ years} , , \quad \tau_3 \approx 6.2 \text{ years}.$$

In this context it is remarkable that Schneider and Gal-Chen (1973) state that, in one of their integrations, the solution of (4) with initial data $\overset{\circ}{u}(x) = \tilde{u}(x)$ and $\mu = 0.984$, after dropping rapidly by about 12 K in average temperature, was nearly constant for about 50 years of simulated time, and then finally dropped to a steady state close to our $u_3(x)$. From our results it becomes clear that the solution mentioned above hovered for a time of the order of τ_2 around u_2 , but could not persist there indefinitely because of the instability of u_2 , and finally attained u_3 , which was stable. *

It also follows from (13) and (14) that multiplying $C(x)$ by a constant $\kappa > 0$ will result in τ_j , $1 \leq j \leq 3$, being multiplied by κ . A similar statement holds also for the nonlinear equation (4), since such a constant κ just corresponds to a different scaling of the time t (see also Schneider and Gal-Chen, 1973). Experiments in determining

* We shall see in the next section that τ_2 increases with decreasing μ .

characteristic response times for solutions of (4') were done by Dwyer and Petersen (1973), who used two heat capacities $C(x)$, both larger than that used by Schneider and Gal-Chen (1973) and by us. It seems, however, that upon decreasing μ in (4) to $\mu = 0.98$, as they always took $\bar{u}(x) = \tilde{u}(x)$ in (5b), the average temperature of the solution $u(x,t)$ dropped rapidly at first, and only slowly thereafter, as indicated by Figure 2 in their article. Apparently this slow decrease, which shows that their solution $u(x,t)$ of (4') was approaching a steady state close to our $u_2(x)$, was interpreted by them as proving the nonexistence of a steady state $u_3(x)$, which had been obtained in the work of Budyko, Sellers and Faegre when decreasing μ by a similar amount.

The influence of changes in μ on the steady-state solutions u_j , $1 \leq j \leq 3$, of (4') will be investigated in the following section. At this point we only want to mention that, whereas a multiplicative factor κ in $C(x)$ affects the magnitude of $\lambda_j^{(1)}$ and hence of τ_j , our theorem shows that it does not affect the actual stability of u_j , i.e., the sign of $\lambda_j^{(1)}$.

6. Perturbed Steady-State Solutions and Bifurcation

It is clear that steady-state solutions of (4') could not spontaneously evolve into each other. More precisely, the solution of (4'-5a) with initial condition $u(x,0) = u_j(x)$, $j = 1,2,3$, is $u(x,t) \equiv u_j(x)$. Moreover, it stands to reason that, for any physical initial condition, $\overset{\circ}{u}(x) \geq 100 \text{ K}$, we would have

$$\lim_{t \rightarrow \infty} u(x,t) = u_j(x) ,$$

with $j = 1$ or $j = 3$, since $u_2(x)$ is (linearly) unstable, whereas $u_1(x)$, $u_3(x)$ are (linearly) stable (and $u_4(x) \leq -170\text{K} < 0$).

Thus, to explain physical ice ages, one has to consider perturbations in the parameters appearing in equation (4'). Such perturbations would presumably be caused by physical mechanisms not included in the model. The most likely candidate for such a role is μ , which up to now was taken to be unity. Indeed, many ice-age theories rely heavily on a change, however small, in the amount of solar radiation reaching the lower layers of the atmosphere (SMIC, 1971, Beckinsale, 1965).

Some attribute the assumed decreases in solar radiation to changes in the parameters of the motions of our planet (Milankovitch, 1930), others to airborne volcanic dust due to an increase in volcanic activity (Fuchs & Patterson, 1947), and so on. There has also been concern about a

possible climatic catastrophe being imminent because of the increase in the quantity of industrial pollutants in the atmosphere (Rasool and Schneider, 1971).

To investigate the effect of such changes in the model at hand, the curve $u_x(1)$ vs. $u(0)$ was recomputed for different values of μ , in particular with a view to obtaining $u_1(x;\mu)$, $u_2(x;\mu)$. One important result is that these two solutions coalesce for

$$\mu_c = 0.98152$$

and disappear entirely for $\mu < \mu_c$. The bifurcating solution $u = u_c(x) = u_1(x;\mu_c) = u_2(x;\mu_c)$ was computed with over-all relative accuracy 10^{-9} and $|u'_c(1)| < 5 \times 10^{-7}$. The $(u(0), u_x(1))$ -curve corresponding to $\mu = \mu_c$ is given in Figure 5; notice that it is very flat near $u(0) = u_c(0)$, which makes it difficult to compute $u_c(x)$ accurately.

Further computations were carried out for $\mu = 0.982, 0.985, 1.01, 1.02, 1.03, 1.04$ and 1.05 . The results of these computations are summarized in Table 3 and plotted in Figure 6. It is quite interesting that, whereas for $\mu \geq 1.0$ the dependence of $u_j(0)$, $\&_{\Delta} u_j(x)$, $j = 1, 2$, on μ is almost linear, this dependence is definitely quadratic near $\mu = \mu_c$; the latter is in good agreement with the general theory of bifurcation for nonlinear parabolic problems (Hoppensteadt and Gordon, 1975). According to the theory, there exists in principle the possibility that, instead of disappearing at $\mu = \mu_c$, the two solution branches $u_1(x;\mu)$, $u_2(x;\mu)$ could

merge into one periodic solution $u_{12}(x,t;\mu)$ for $\mu < \mu_c$. This possibility was not borne out, however, by the time-dependent computations of Dwyer and Petersen (1973), and of Gal-Chen and of Schneider (1973, 1975); we did not investigate it further.

Concerning the problem of the pole-to-equator temperature gradient,

$$\Delta u_j = u_j(1) - u_j(0) , \quad 1 \leq j \leq 3,$$

as discussed by Stone (1973) and Gal-Chen and Schneider (1975), the curve $\Delta u_j = \Delta u_j(\mu)$, $j = 1, 2$, is particularly interesting. We notice that

- (a) the values of Δu_1 lie below those for Δu_2 ;
- (b) the values of Δu_1 are monotonically decreasing with μ ;
- (c) the values of Δu_2 have a maximum for μ somewhere between $\mu = 0.985$ and $\mu = 0.99$;
- (d) the dependence of both Δu_1 and Δu_2 on μ , but especially that of Δu_1 , is very steep near $\mu = \mu_c$.

Being aware of the limitations of the model, as pointed out in Section 2, we do not want to make extensive comments concerning these results, but only note them for comparison with the results of other models and for further study.

We also studied the stability of the solutions $u = u_c(x)$ and $u = u_3(x;\mu_c)$. Repeating the construction indicated at the beginning of Subsection 5b for $v = v_c$ and $v = v_3$, where

$$L_j = - \frac{\partial}{\partial u} N(u; \mu_c) \big|_{u=u_j}, \quad j = c, 3,$$

we obtained the following results:

- (a) v_j , $j = c, 3$, is positive, $v_j \geq V_j > 0$, $v_j \geq 0.75$;
- (b) $\frac{d}{dx} v_c(1) = -7.56 \times 10^{-3}$, $\frac{d}{dx} v_3(1) = 4.23362$.

Clearly $u_3(x; \mu_c)$ is still stable, in fact $(d/dx)v_3(1; \mu_c) = 4.23$ is very close to $(d/dx)v_3(1; 1.0) = 4.31$, showing the extremely smooth dependence of $u_3(x; \mu)$ on μ .

The negativity of $(d/dx)v_c(1)$ would seem to point to outright instability of $u_c(x)$, but in fact its small numerical value indicates that, within the accuracy of the computations, it is actually zero, i.e., $u_c(x)$ is neutrally stable. Indeed, the mathematical theory of nonlinear problems (Nirenberg, 1974) shows that for a bifurcation to exist, as in the case at hand, the linearization

$$L_c = - \frac{\partial}{\partial u} N(u; \mu_c) \big|_{u=u_c}$$

of the spatial, time-independent, operator N at the bifurcation point (u_c, μ_c) has to have a zero eigenvalue. This follows from the infinite-dimensional generalization of the one-dimensional fact that a function can be inverted in a neighborhood of a point at which it has a nonzero derivative, i.e., that it has a unique branch near such a point.

We also computed the lowest eigenvalues $\lambda_j^{(1)}$ and corresponding eigenfunction $w_j^{(1)}$ of $L_j(\mu_c)$ for $j = c, 3$,

by the shooting method described in Subsection 5b. In this computation, the results on v_j mentioned before were valuable in making a first guess for the shooting parameter λ . The computations yielded

$$\lambda_c^{(1)} = -1.287 \times 10^{-11}, \quad \lambda_3^{(1)} = 5.07265 \times 10^{-9}.$$

Again we notice that $\lambda_3^{(1)}(\mu_c) = 5.07 \times 10^{-9}$ is very close to $\lambda_3^{(1)}(1.0) = 5.13 \times 10^{-9}$, whereas $|\lambda_c^{(1)}| \approx 0.4 \times 10^{-2} \lambda_1^{(1)}(1.0) \approx 0.2 \times 10^{-2} \lambda_2^{(1)}(1.0)$ is practically zero, as it has to be analytically.

It is clear by the continuity of $\lambda_j^{(1)}(\mu)$ in the parameter μ that for $\mu_c < \mu \leq 1.05$ we have $\lambda_1^{(1)} > 0$, $\lambda_3^{(1)} > 0$, and $\lambda_2^{(1)} < 0$, so that the interglacial and the ice-covered earth are stable for the entire range of μ explored, whereas the glacial is unstable for the same range of μ . Furthermore the ice-covered earth is stable also for smaller μ .

There is one further point of view, which, while illuminating the significance of the neutral stability of $u_c(x)$, also argues for our linear stability analysis being sufficient for concluding on nonlinear stability or instability of the steady-state solutions of (4') corresponding to different values of μ . This viewpoint has to do with the existence of a variational principle for (4'). Indeed

$$N(u; \mu) = 0$$

is the Euler-Lagrange equation for the extrema of the functional

$$J(u; \mu) = \int_0^1 \left\{ p u_x^2 + r G(x, u) \right\} dx;$$

here p, r are given by (17b,c) and

$$G(x,u) = \int F(x,\omega) d\omega ,$$

where $F(x,u)$ is defined by (7d).

Clearly the stable solutions $u_1(x;l)$, $u_3(x;l)$ correspond to local minima of $J(u;l)$, whereas $u_2(x;l)$ is a local maximum. As $u_1(x;\mu)$, which is a minimum for $\mu > \mu_c$, coalesces with $u_2(x;\mu)$, which is a maximum for $\mu > \mu_c$, at $\mu = \mu_c$, a saddle point $u = u_c(x)$ obtains, whereas $u_3(x;\mu_c)$ is still a minimum.

This variational interpretation makes it very plausible that solutions $u(x,t;\mu)$ of the "flow"

$$u_t = N(u;\mu) , \quad \mu > \mu_c ,$$

with initial conditions near $u_j(x;\mu)$, that is at a finite but small, rather than infinitesimal, distance from $u_j(x;\mu)$, $j = 1,2,3$, will tend as $t \rightarrow \infty$ towards u_j if u_j is a minimum, i.e., $j = 1,3$, and away from it when u_j is a maximum, i.e., $j = 2$. Similarly, for $\mu = \mu_c$, solutions starting near $u_3(x;\mu_c)$ will still converge to u_3 , but solutions starting near $u_c(x)$, though they may hover for a long time near u_c , since $\tau_1, \tau_2 \rightarrow \infty$ as $\mu \rightarrow \mu_c$, will eventually move away from it, along a negative slope of the saddle, and finally tend towards the absolute minimum u_3 . This seems a rather satisfactory, although heuristic, explanation of the results of the time-dependent computations of Dwyer and Petersen (1973) and of Schneider and Gal-Chen (1973), which we mentioned already in Section 5.

7. Concluding Remarks

We studied the zonally-and-vertically averaged energy-balance climate model governed by equations (1-3); these equations are based on simple parameterizations of albedo, greenhouse effect and eddy diffusion of heat in terms of yearly averaged sea-level temperature, which is the only dependent variable of the model.

Three positive steady-state solutions of the model, symmetric with respect to the equator, were found by accurate numerical computations, and apparently no more such solutions exist. These steady states can be identified with an interglacial climate, approximating very well the one prevailing presently on earth, a glacial climate, and a climate during which the earth would be completely ice covered. The climates obtained were only slightly changed when making small changes in the numerical values of the coefficients and when making certain changes in the functional form of the model's equations. However, the bounds on the values the albedo can take were essential in order to obtain these three climates; also linearizing the outgoing planetary radiation resulted in a reduction of the number of solutions.

We then determined the stability of the time-dependent solutions of (1') under small perturbations about the model's steady states. This stability was shown to depend on certain properties of a comparison function, which was constructed numerically.

We found that the interglacial and the "deep freeze" climate are stable, and that the glacial climate is unstable. This means that the first two can obtain, at least approximately, as steady states in a physical system governed by equations very similar to (1-3), but that the latter cannot; the same is true about these climates as limiting steady states for time-dependent numerical solutions of such equations.

We further showed how changes in an important parameter, the average intensity of the solar radiation, influence the steady-state solutions of the model. The dependence on this parameter of all steady states was shown to be gradual and smooth for increases of up to 5% and decreases of up to about 2%. However for a critical value of the parameter, equal to 98.15% of its present value, the glacial and interglacial climates coalesced and they disappeared entirely for smaller values of the parameter, leaving the ice-covered earth as the only possible stable, steady climate of the model.

This result is important, as it stresses the difference between the stability of a steady state with respect to the time evolution of a physical system governed by a given, fixed equation, and the stability of a steady state with respect to changes in a parameter, which determines the behavior of the system. For definiteness, let us call the former internal stability and the latter external stability; we have shown that the "deep freeze" is stable for our system

both internally and externally, that the glacial is unstable in both senses, and that the interglacial, or "present climate," is internally stable, but externally unstable.

The limitations of equations (1-3) as a model for the description of the long-term behavior of the atmosphere-ocean-cryosphere system, and of energy-balance models in general, have been discussed extensively. Because of these limitations, we believe that the results above should not be taken at face value as statements about the climate of our planet. These results, however, seem to clarify the physical content and mathematical properties of such models. Also, the methods used here could be helpful in investigating other models, which will include more elaborate and reliable parameterizations of the physical phenomena governing climate. We further hope that insight gained into the behavior of solutions of a certain type of model will advance the formulation of other models, and that these will come closer to explaining past changes in climate and predicting future changes.

References

- [1] Beckinsale, R. P., 1965. Climatic change, in Essays in Geography for Austin Miller, edited by J. B. Whittow and P.D. Wood, University of Reading, England, pp. 1-38.
- [2] Birkhoff, G., and G.-C. Rota, 1969. Ordinary Differential Equations, Blaisdell, Waltham, Mass., 366 pp.
- [3] Budyko, M. I., 1969. The effect of solar radiation variations on the climate of the Earth, Tellus 21, 611-619.
- [4] Courant, R., and D. Hilbert, 1953. Methods of Mathematical Physics, Volume I, Wiley-Interscience, New York, 560 pp.
- [5] Dwyer, H. A., and T. Petersen, 1973. Time-dependent global energy modeling, J. Appl. Meteor. 12, 36-42.
- [6] Faegre, A., 1972. An intransitive model of the earth-atmosphere-ocean system, J. Appl. Meteor. 11, 4-6.
- [7] Fuchs, V. E., and T. T. Paterson, 1947. The relation of volcanicity and orogeny to climatic change, Geological Magazine 84, 321-333.
- [8] Gal-Chen, T., and S. H. Schneider, 1975. Energy-balance climate modeling: Comparison of radiative and dynamic feedback mechanisms, Tellus (to appear).
- [9] Handbook of Meteorology, F. A. Berry, Jr., E. Bollay, N. R. Beers, editors, 1945. McGraw-Hill, New York, pp. 342-345.

- [10] Held, I. M., and M. J. Suarez, 1974. Simple albedo feedback models of the ice caps, Tellus 26, 613-629.
- [11] Hindmarsh, A. C., 1972. Linear Multistep Methods for Ordinary Differential Equations: Method Formulations, Stability, and the Methods of Nordsieck and Gear, UCRL-51186, Rev. 1, Lawrence Livermore Laboratory, University of California, Livermore, CA 94550.
- [12] _____, 1974. GEAR: Ordinary Differential Equation System Solver, UCID-30001, Rev. 3, Lawrence Livermore Laboratory, University of California, Livermore, CA 94550.
- [13] Hoppensteadt, F., and N. Gordon, 1975. Nonlinear stability analysis of static states which arise through bifurcation, Comm. Pure Appl. Math. 28 (to appear).
- [14] Isaacson, E., and H. B. Keller, 1966. Analysis of Numerical Methods, John Wiley & Sons, New York, 541 pp.
- [15] Jackson, J. D., 1962. Classical Electrodynamics, John Wiley & Sons, New York, p. 611.
- [16] Keller, H. B., 1968. Numerical Methods for Two-Point Boundary Value Problems, Blaisdell, Waltham, Mass., 184 pp.
- [17] Lorenz, E. N., 1968. Climatic determinism, in Causes of Climatic Change, Meteor. Monoqr. 8, No. 30, 1-3.
- [18] _____, 1970. Climatic change as a mathematical problem, J. Appl. Meteor. 9, 325-329.

- [19] Leith, C., 1974. Manuscript.
- [20] Milankovitch, M., 1930. Mathematische Klimalehre und astronomische Theorie der Klimaschwankungen, in Handbuch der Klimatologie, edited by W. Köppen and R. Geiger, Vol. 1A, Berlin.
- [21] Nirenberg, L., 1974. Topics in Nonlinear Functional Analysis, CIMS Lecture Notes, New York Univ., N.Y., 259 pp.
- [22] Rasool, S. I., and S. H. Schneider, 1971. Atmospheric CO₂ and aerosols: Effects of large increases on global climate, Science 173, 138-141.
- [23] Robinson, G. D., 1971. Review of climate models, in Man's Impact on the Climate, edited by W. H. Matthews, W. W. Kellogg and G. D. Robinson, MIT Press, Cambridge, Mass., pp. 205-215.
- [24] Schneider, S. H., and T. Gal-Chen, 1973. Numerical experiments in climate stability, J. Geophys. Res. 78, 6182-6194.
- [25] Sellers, W. D., 1969. A global climatic model based on the energy balance of the earth-atmosphere system, J. Appl. Meteor. 8, 392-400.
- [26] _____, 1973. A new global climatic model, J. Appl. Meteor. 12, 241-254.
- [27] SMIC (Study of Man's Impact on the Climate), 1971. Inadvertent Climate Modification, MIT Press, Cambridge, Mass., 308 pp.
- [28] Stone, P. H., 1973. The effect of large-scale eddies on climatic change, J. Atmos. Sci. 30, 521-529.

Table Captions

Table 1. Empirical functions appearing in equation (4).

The functions Q , b , z are based on data in Tables 1 and 2 of Sellers (1973). The functions C , k_1 , k_2 are based on data provided by Dr. T. Gal-Chen (1974, personal communication), and used in the (SV) model of Schneider and Gal-Chen (1973).

Table 2. Influence of different modifications in the model's

equation (4) on the number of steady-state solutions and the numerical values of these solutions. The existing solutions are identified by the temperature at the pole, $u_j(0)$, $j = 1, 2, 3$. In case a solution is missing, this is indicated by (-) in the corresponding row-and-column location. S stands for the coefficients being fitted by cubic splines, B for Bernstein polynomials. A downward arrow (\downarrow) to the right of a comment indicates that the equation used in the numerical experiments reported in all subsequent rows had the feature pointed out in that comment. Otherwise comments refer only to the row in which they appear. A left arrow, $x \leftarrow y$, means that the quantity x was replaced in the equation by the quantity y . The entries given with less than five decimal digits resulted from computations with lower precision than indicated in the text.

Table 3. Dependence of the steady states $u_1(x;\mu), u_2(x;\mu)$ on the normalized average intensity of the solar radiation, μ . The columns give $u(0)$, the temperature at the pole, \bar{u} , the average temperature, and $\Delta u = u(1) - u(0)$, the pole-to-equator temperature difference for u_1 and for u_2 respectively. The values for $\mu_c = 0.98151822$ correspond to the bifurcating steady state $u = u_c(x)$.

ϕ	u	C	Q	b	z	k_1	k_2
1 deg	1 deg K	1 cal $\cdot \text{cm}^{-2} \text{deg}^{-1}$	10^{-2} cal $\cdot \text{cm}^{-2} \text{sec}^{-1}$	1	1 m	$10^{-5} \text{ cal deg}^{-1}$ $\cdot \text{cm}^{-2} \text{sec}^{-1}$	$10^{-2} \text{ cal dyn}^{-1}$ $\cdot \text{sec}^{-1}$
0	247.3625	500	0.426	2.192	1204.5	0.47113	0
5							
10	252.0740	1000	0.440	2.960	820.0	0.61988	0.9314
15							
20	262.5715	1500	0.484	2.934	295.0	1.19933	1.9772
25							
30	271.2980	4725	0.579	2.914	150.5	1.50214	3.4348
35							
40	278.9325	5625	0.696	2.915	193.5	1.51063	4.8316
45							
50	285.7530	5812	0.804	2.868	301.0	1.69562	3.7359
55							
60	291.4090	5813	0.894	2.821	261.0	2.02342	0.6903
65							
70	296.0815	5625	0.961	2.804	133.5	3.20611	-2.5401
75							
80	298.7815	6000	1.003	2.805	156.0	4.80401	-10.5975
85							
90	299.3510	5625	1.017				

Table 1

$u_3(0)$	$u_2(0)$	$u_1(0)$	Comments
168.94	223.97	247.74	S, Sellers α , full eq., $k = k(x, u)$
169.44	227.76	247.55	S, " " $k = k(x, \tilde{u})$
-	-	259.26	S, " , $R_0 = 0.61 \sigma \tilde{u}^3 [\tilde{u} - 4(u - \tilde{u})]$, $k = k(x, \tilde{u})$
169.0	222.6	238.5	S, " $k = k_1(x) \downarrow$
170.0	229.75	238.04	B, "
-	229.2	238.04	B, " $\alpha \not\leq 0.85$
168.0	-	-	S \downarrow , " $m = 0$ (no greenhouse effect) $\alpha \leq 0.85 \downarrow$
170.0	222.0	245.0	Sellers α , $c_2 = 0 \downarrow$, $m = 0.5 \downarrow$
170.0	222.0	-	Faegre $\alpha \downarrow$, $\alpha \not\geq 0.25$
170.0	222.0	255.0	$\alpha \geq 0.25 \downarrow$
169.0	232.0	265.0	$b(x) \leftarrow \epsilon_{\Delta} b(x) = 2.85881 \downarrow$
-	-	-	$c(x, u) \leftarrow 0$ (no infrared radiation)
160.0	-	-	$v \cot \frac{\pi x}{2} \leftarrow 0$ (no singularity)
170.0	250.0	280.0	$k(x, \tilde{u}) \leftarrow \epsilon_{\Delta} k(x, \tilde{u}(x)) \equiv K_0 = 2.2 \times 10^{-5} \downarrow$
165.0	-	-	$v \cot \frac{\pi x}{2} \leftarrow 0$
-	-	-	$c(x, u) \leftarrow 0$
-	247.36	-	$R_0 = \epsilon_{\Delta} c(x, \tilde{u}(x)) \sigma \tilde{u}^4(x) = 5.63 \times 10^{-3}$
193.27	233.95	277.79	$R_0 = 0.61 \sigma u^4$ ($\epsilon_{\Delta} c(x, \tilde{u}(x)) = 0.61$) \downarrow
190.0	232.0	280.0	$v \frac{\pi}{2} \cot \frac{\pi x}{2} \leftarrow \frac{v}{x}$
197.0	249.0	295.0	$Q(x) \leftarrow \epsilon_{\Delta} Q(x) = 8.333 \times 10^{-3}$
190.0	238.0	275.0	$b(x) \leftarrow \epsilon_{\Delta} b(x) + c_1 c_2 \epsilon_{\Delta} z(x) = 2.87334$
192.88	232.08	276.06	$k(x, \tilde{u}) \leftarrow K'_0 = 1.96 \times 10^{-5}$

Table 2

	u(0)		$\varepsilon_{\Delta} u$		Δu	
μ	1	2	1	2	1	2
0.98	-		-		-	
0.98151822	235.70000		277.66799		56.34051	
0.982	236.52729	234.88088	279.38752	275.83481	55.77861	56.66504
0.985	240.87022	231.38910	282.14639	273.08646	54.81134	56.88813
0.99	243.74295	229.55772	284.55785	270.91707	53.94044	56.89193
1.00	247.55398	227.76190	287.69906	268.60379	52.80968	56.62315
1.01	250.45869	226.83077	290.06384	267.24989	51.98363	56.15496
1.02	252.94187	225.95469	292.07316	265.95849	51.30562	55.68122
1.03	255.16237	225.11901	293.86462	264.71403	50.72267	55.22456
1.04	257.19489	224.31508	295.50286	263.50733	50.20914	54.76978
1.05	259.08295	223.54529	297.02543	262.34160	49.74993	54.32089

Table 3

Figure Captions

Figure 1

Comparison of curve fitting by (i) Bernstein polynomial approximation, indicated by a dash-dot line, and by (ii) cubic spline interpolation, indicated by a solid line. Bernstein polynomials are not interpolatory and they are variation diminishing, i.e., they have the property of smoothing out the data; this results in a rather poor approximation. Cubic splines are not variation diminishing and they are very good approximants.

Figure 1a

For a very smooth function, like $\tilde{u}(x)$, the two approximation procedures yield curves very close to each other.

Figure 1b

For a function of large total variation, like $k(x, \tilde{u}(x))$, the two procedures yield curves which can differ pointwise by as much as 50 percent of the average value.

Figure 2

Numerically obtained values of $u_x(1; u_0)$ as a function of $u_0 = u(0)$.

Figure 2a

Comparison of the results for equations (7), in which $k = k(x, u)$, with those for equations (7'), in which $k = k(x, \tilde{u}(x))$; the results for (7) are indicated by a solid line, those for (7') by a dash-dot line.

Figure 2b

Results of (7') for $-1330\text{K} \leq u(0) \leq 300\text{ K}$. Notice that as $u_0 = u(0)$ tends towards the ends of the interval, $u_x(1;u_0) \rightarrow +\infty$. The solution $u_4(x)$, corresponding to the negative root of this curve, $u_0 = -186\text{ K}$, does not have a physical significance.

Figure 3

Comparison of the solutions of (4), indicated by a solid line, with those of (4'), indicated by a dash-dot line. The circles indicate mesh data for $u = \tilde{u}(x)$.

Figure 3a

Values of the solutions $u_j(x)$, $j = 1, 2, 3$, for (4) and for (4'). The respective values for $j = 1, 3$ are practically indistinguishable, whereas for $j = 2$ a slight difference exists between the solution of (4) and that of (4').

Figure 3b

Values of the derivatives $\frac{d}{dx} u_j(x)$, $j = 1, 2, 3$, for (4) and for (4'). The differences are larger than in the function values themselves.

Figure 4

The first eigenfunctions, $w_j^{(1)}(x)$, $j = 1, 2, 3$, of
$$L_j = - \frac{\partial}{\partial u} N(u) \Big|_{u=u_j}.$$

Figure 5

The function $u_x(1;u_0)$, obtained by integrating (7') numerically with $\mu = \mu_c$ and with different values of u_0 , $u_0 = u(0) \geq 120\text{ K}$.

Figure 6

Dependence of the solutions $u_j(x;\mu)$, $j = 1, 2$, on the parameter μ . The two plots for $u_j(0)$, $\epsilon_{\Delta} u_j$ are very similar; the plot for $\Delta u_j = u_j(1) - u_j(0)$ is rather different, although it exhibits the same behavior in the neighborhood of the critical point c . The circles indicate the values actually computed, for $\mu = \mu_c$, 0.982, 0.985, 0.99, 1.00, 1.01, 1.02, 1.03, 1.04, 1.05. The letter c distinguishes the values of the plotted quantities $u_j(0)$, $\epsilon_{\Delta} u_j$, Δu_j corresponding to the bifurcating solution $u = u_c(x)$.

Figure 7

The bifurcating solution $u = u_c(x)$. Notice that the ice line, which corresponds to $u = 273$ K, is at about 45° lat. for this solution, i.e., an ice cover extending beyond this latitude would eventually cover the entire earth.

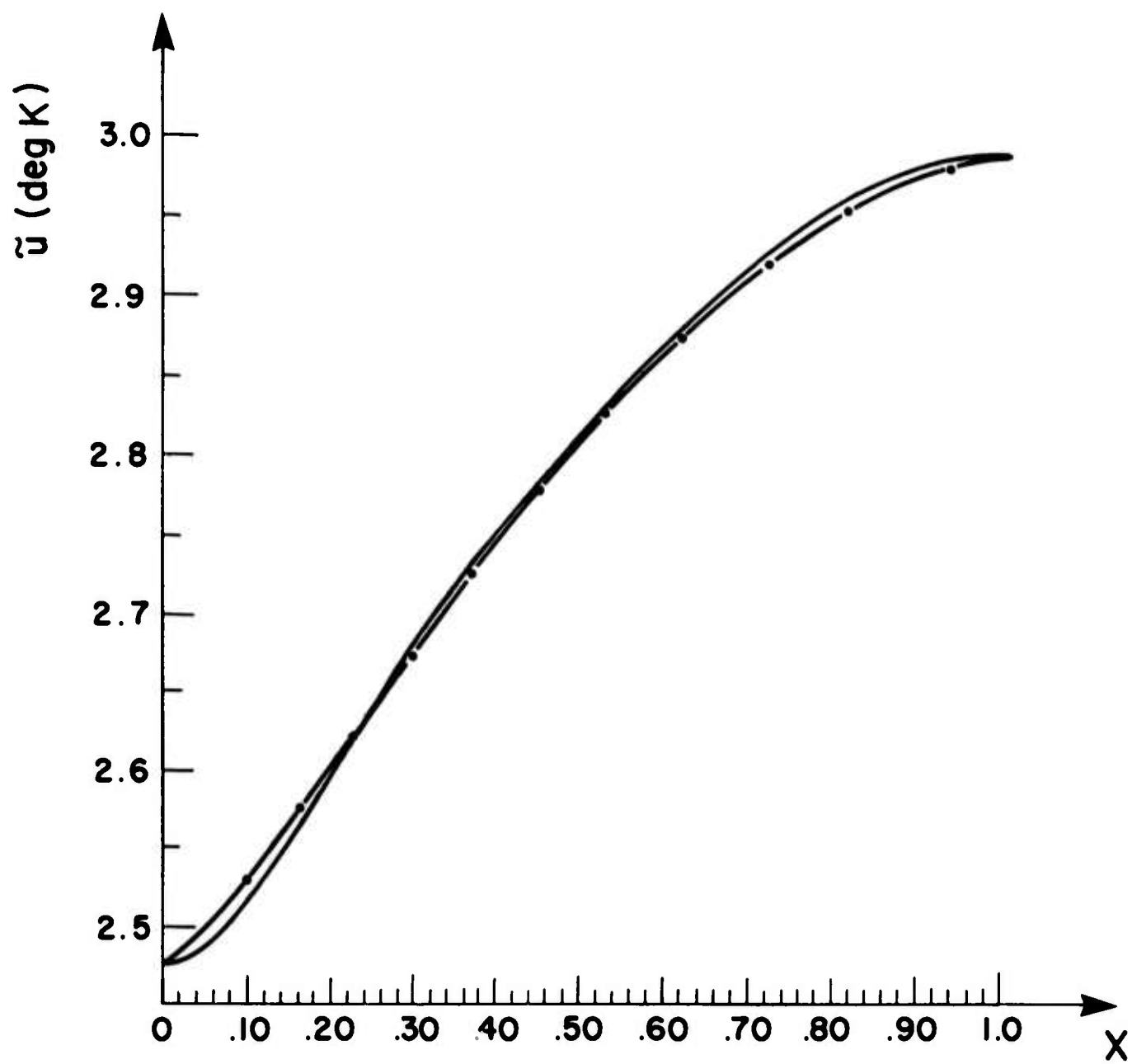


fig. 1a

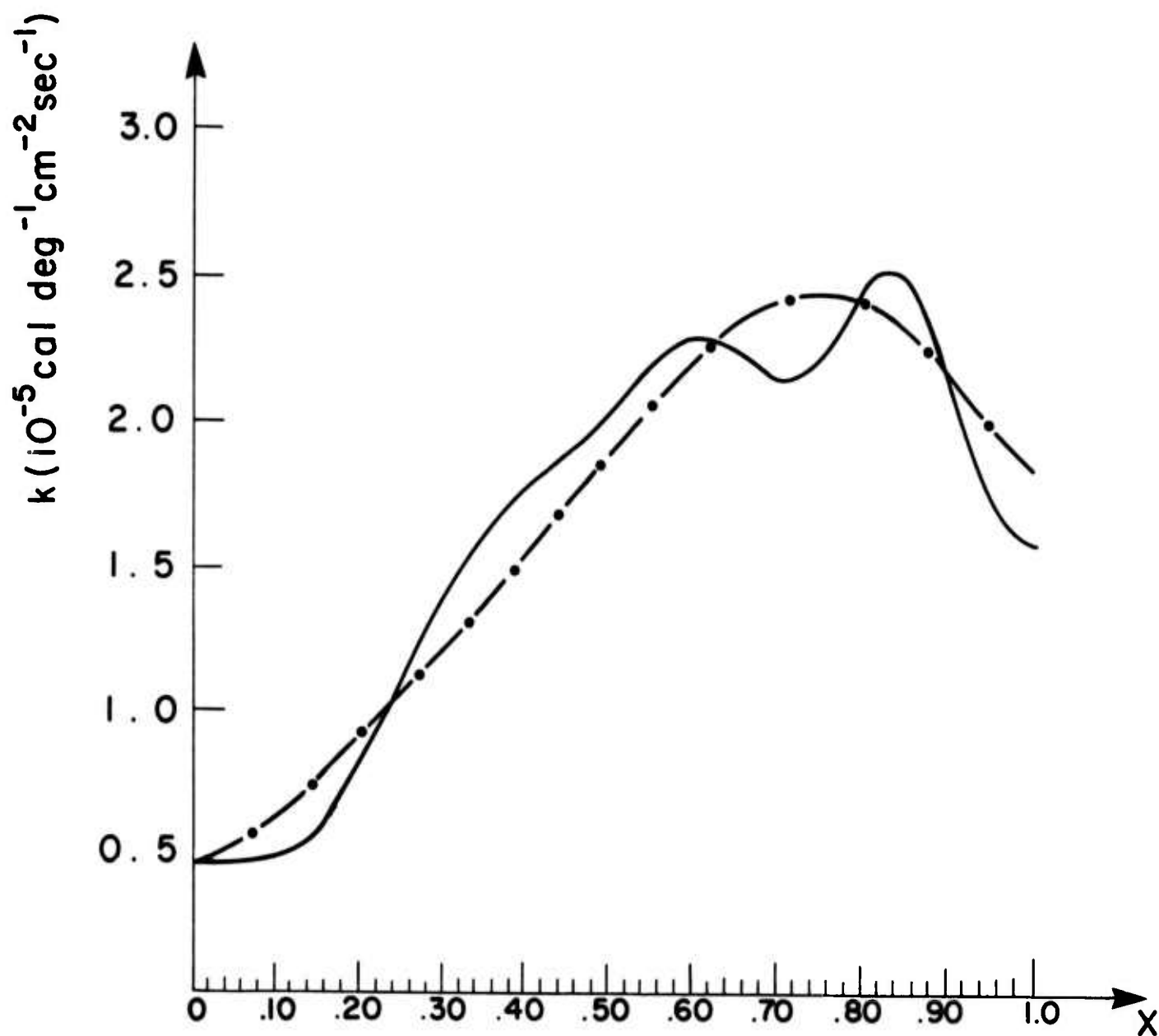
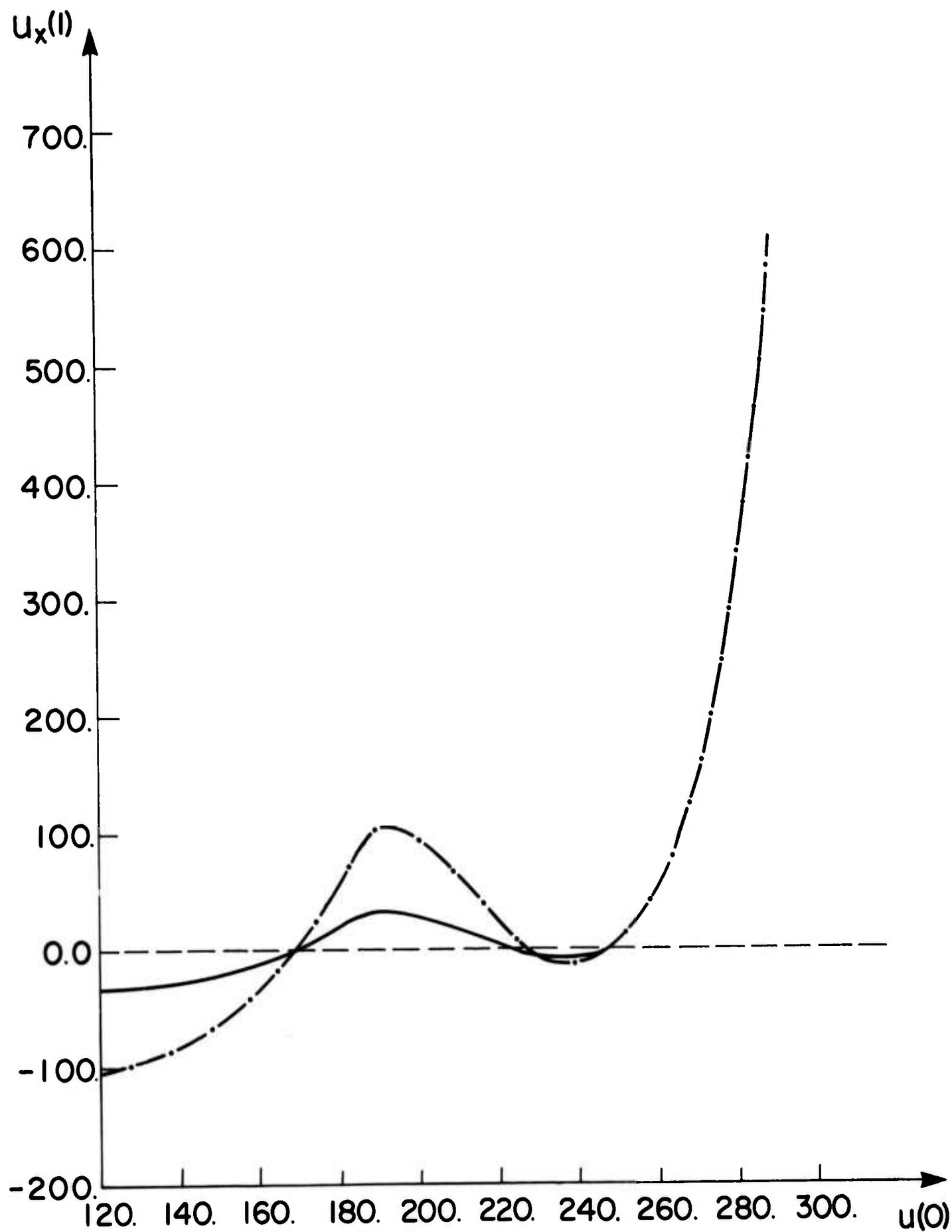


fig. 1b

fig. 2a



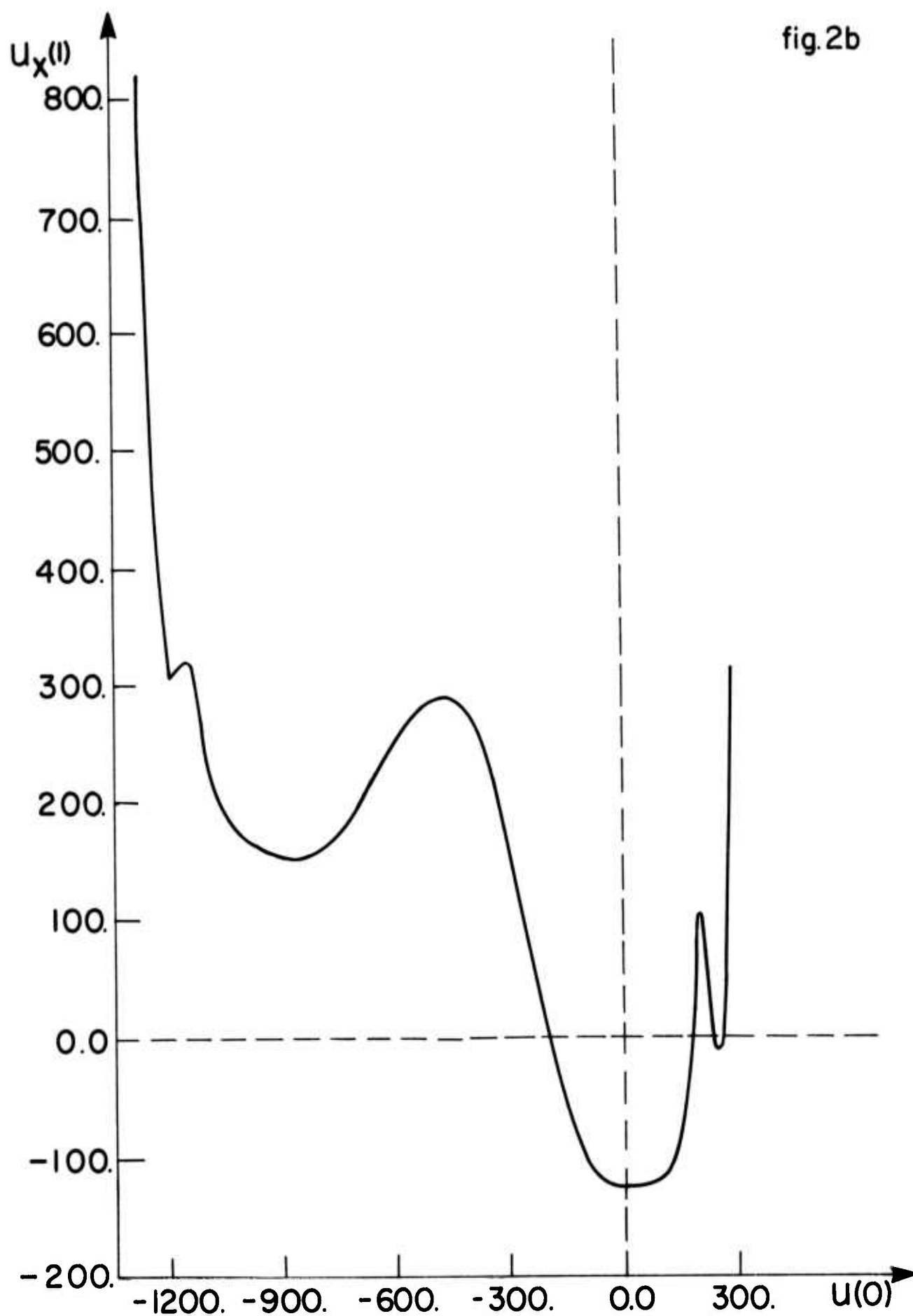


fig. 3a

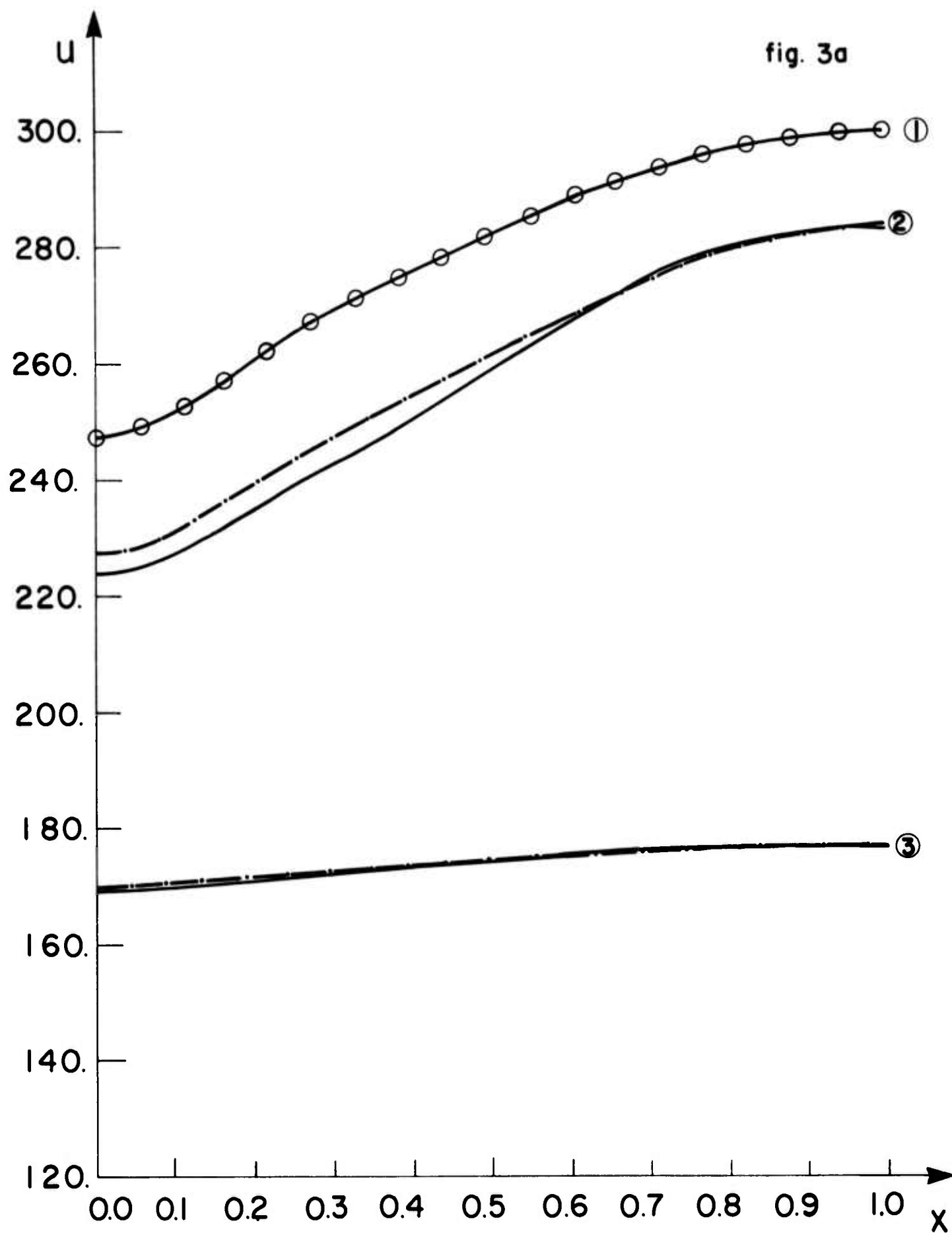
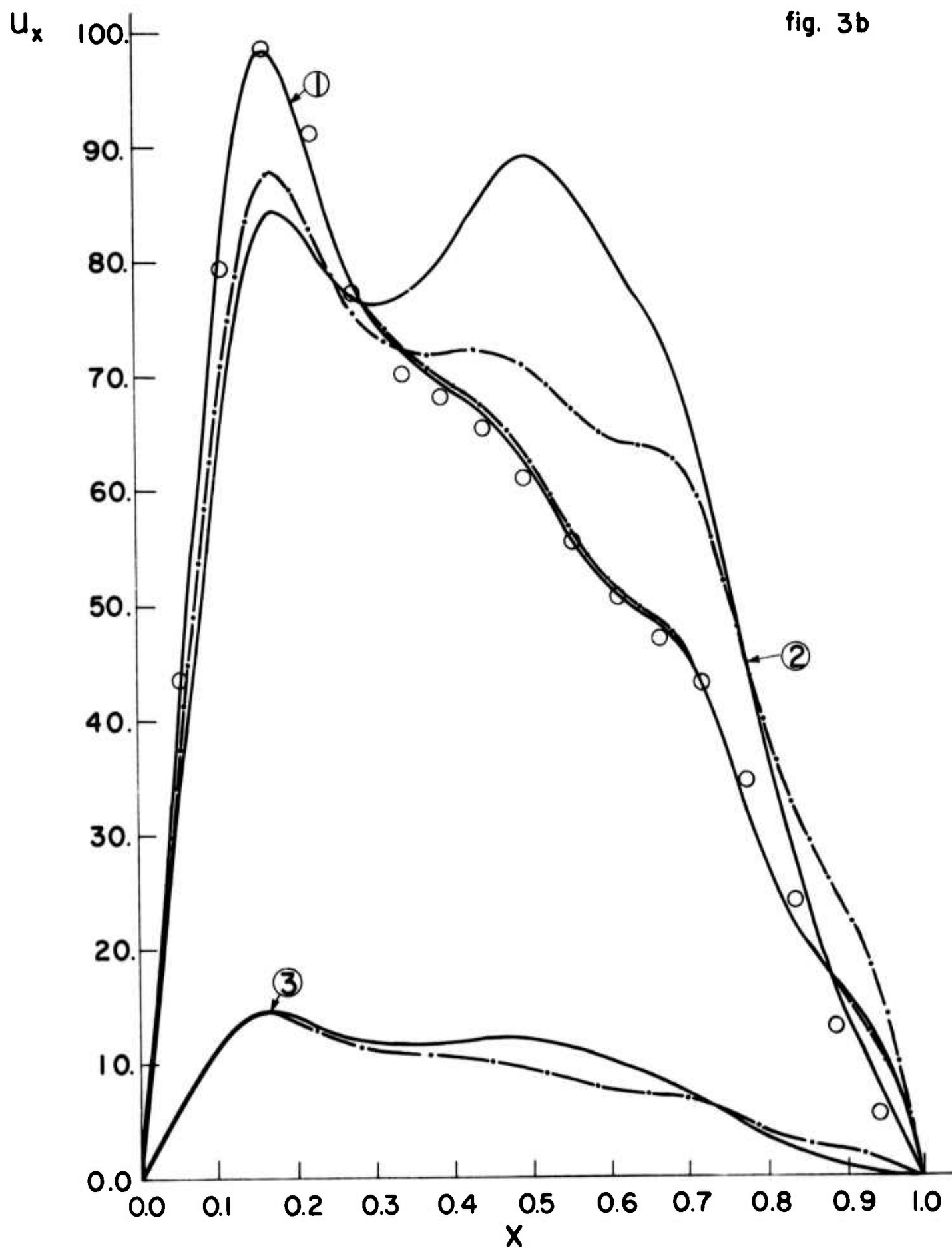


fig. 3b



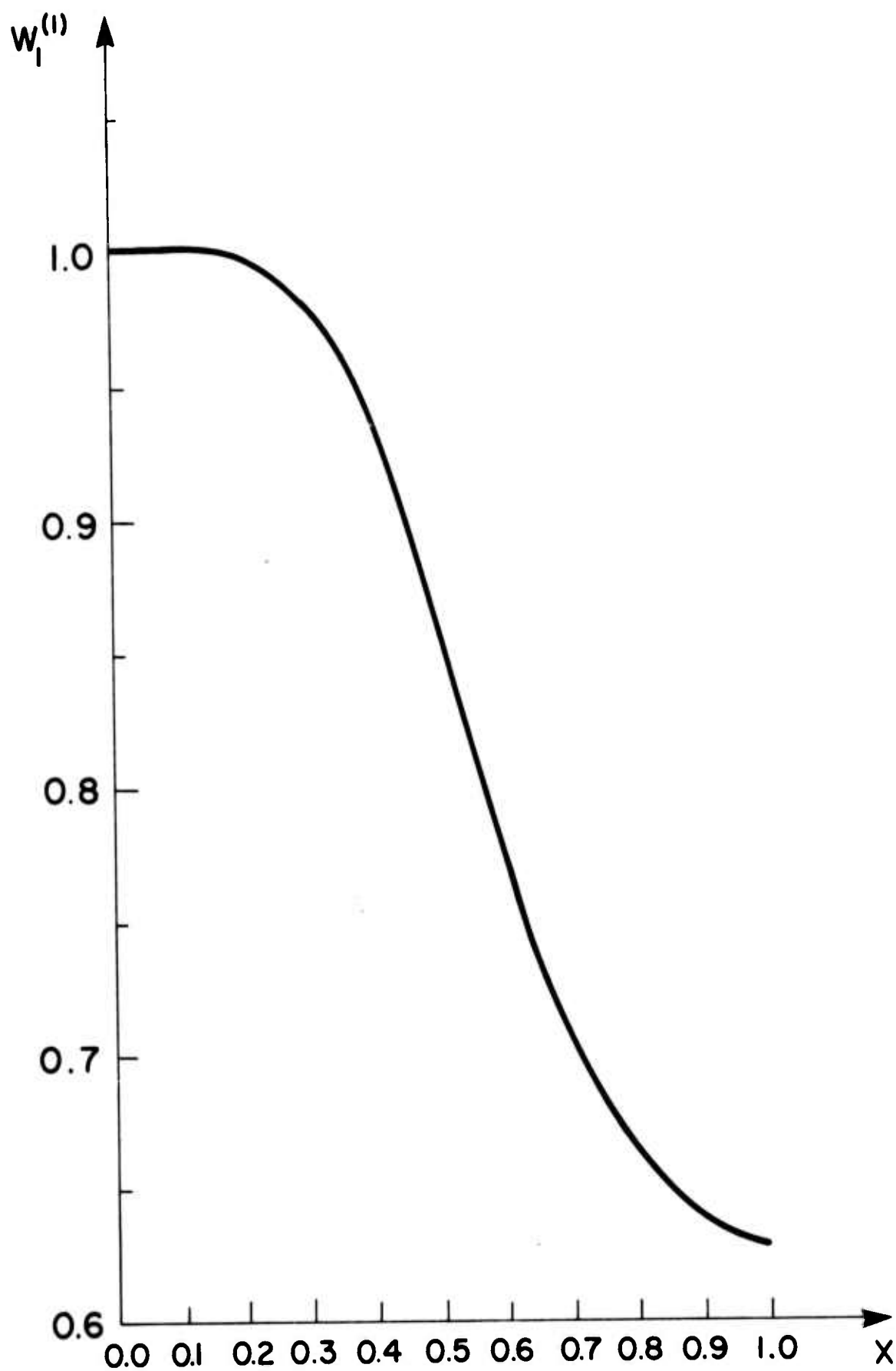


fig. 4a

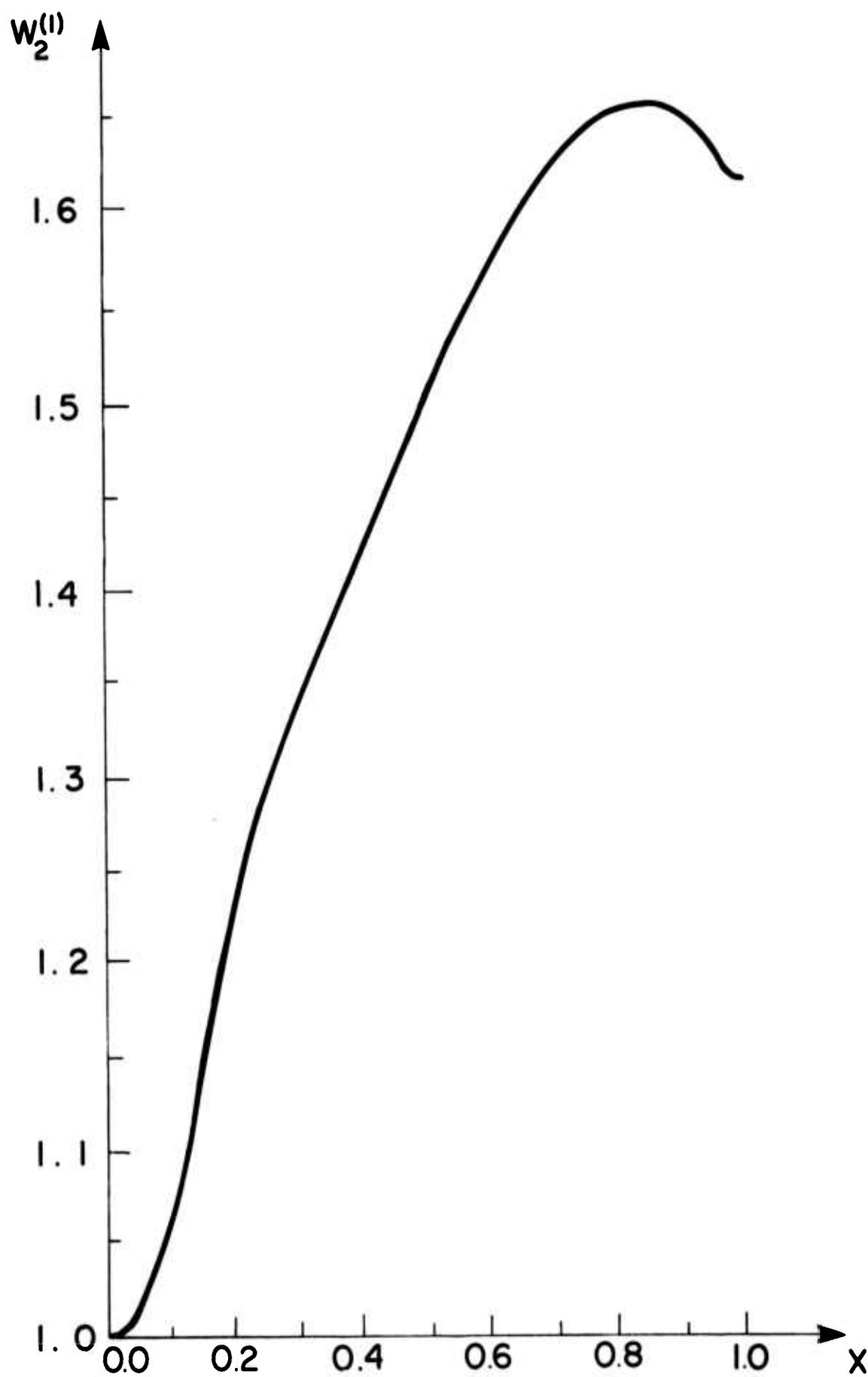


fig. 4b

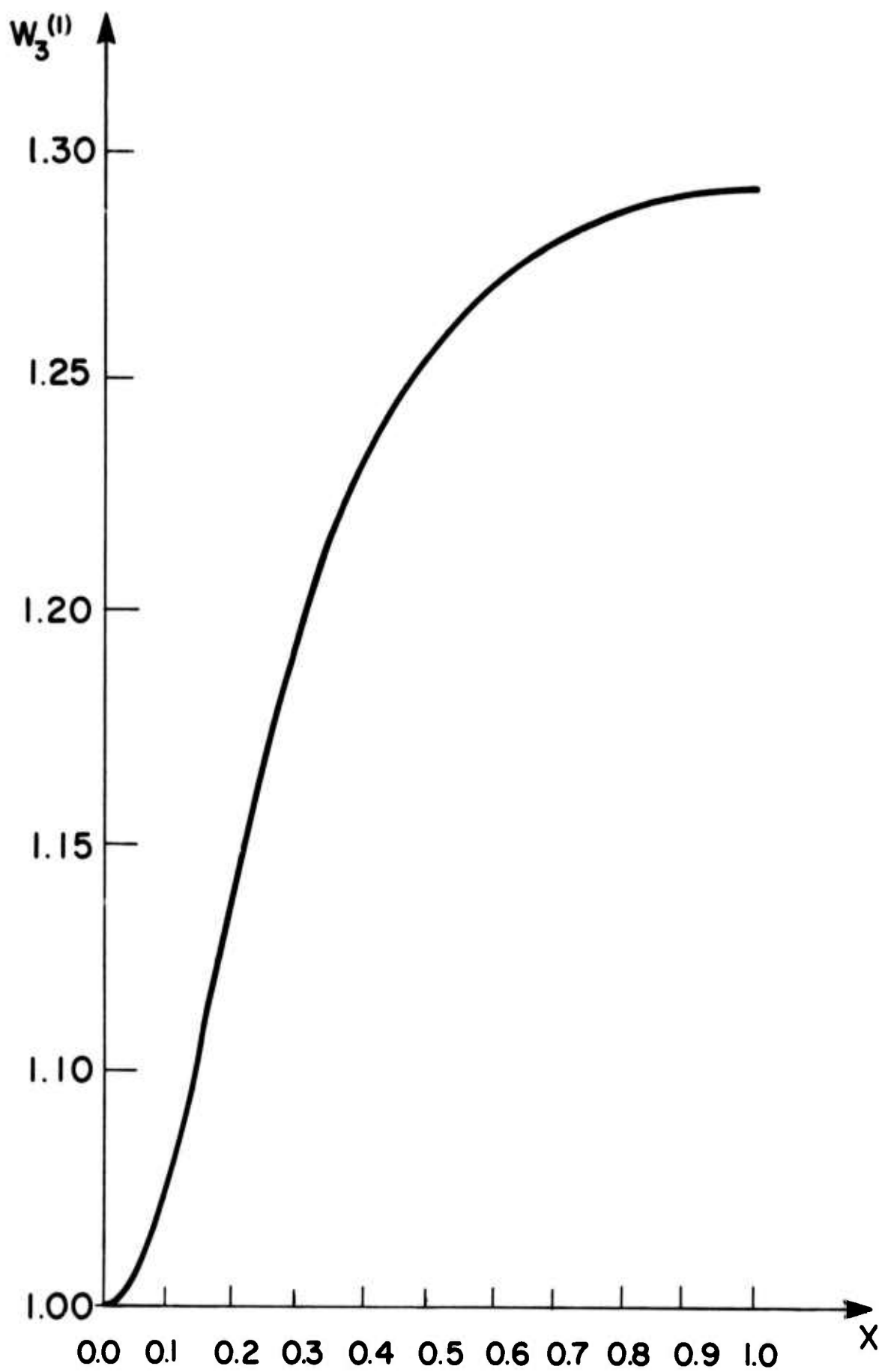


fig. 4c

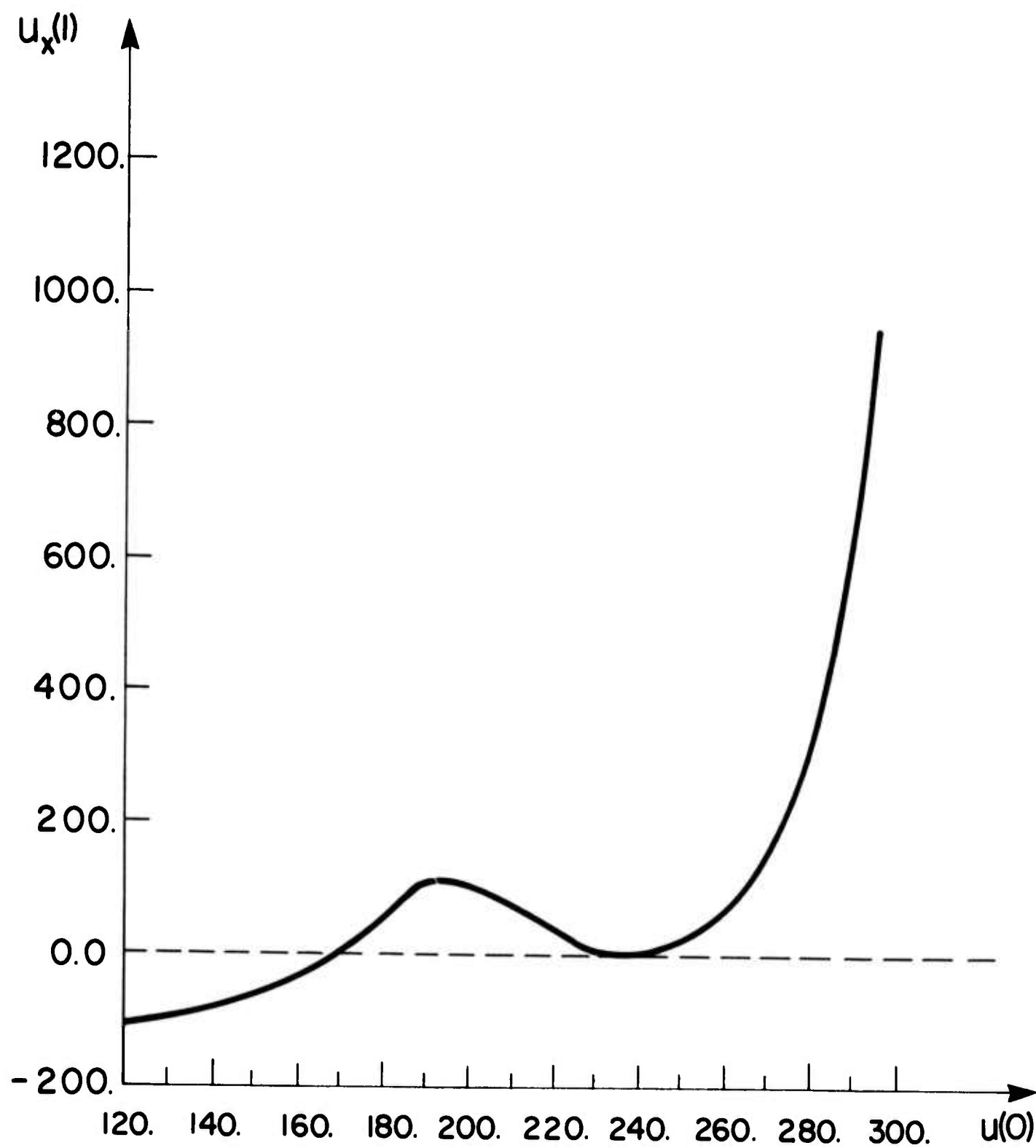


fig. 5

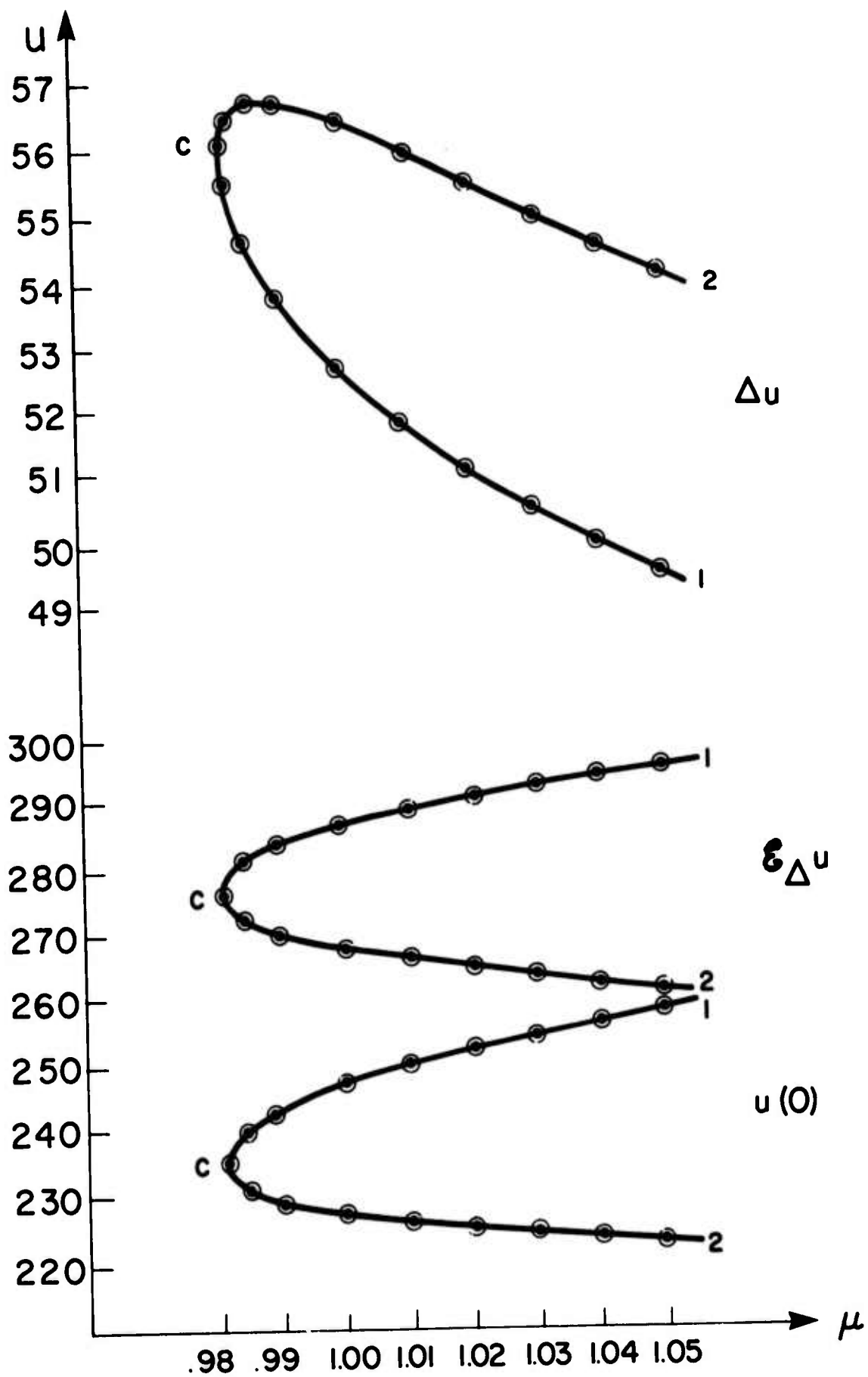


fig. 6

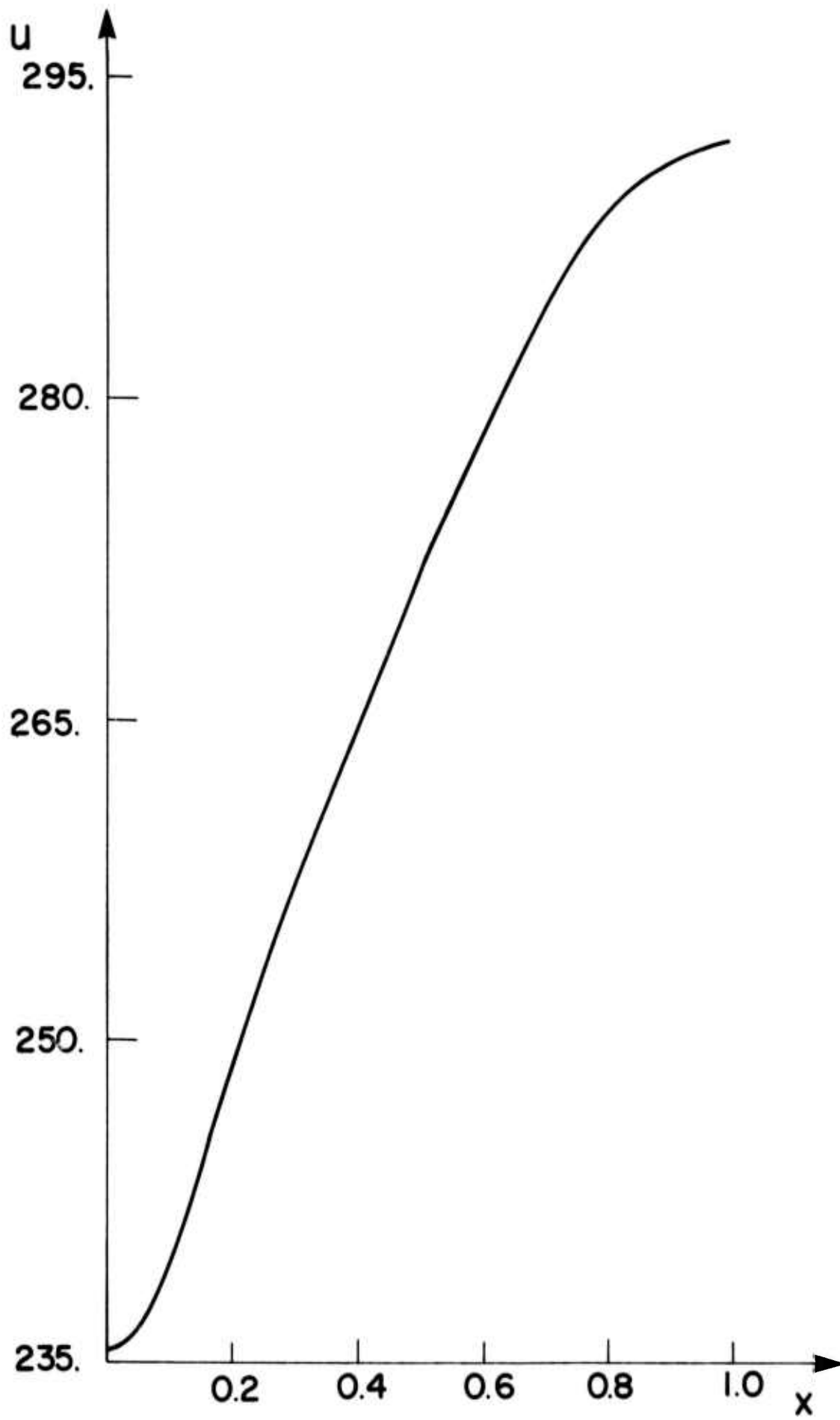


fig. 7